© 2022. Published by The Company of Biologists Ltd | Development (2022) 149, dev200272. doi:10.1242/dev.200272

RESEARCH ARTICLE

Presenilin enhancer 2 is crucial for the transition of apical progenitors into neurons but into not basal progenitors in the developing hippocampus

Yingqian Xia[1], Yizhi Zhang[1], Min Xu[2], Xiaochuan Zou[1], Jun Gao[2,*], Mu-Huo Ji[3,*] and Guiquan Chen[1,4,*]

ABSTRACT

Recent evidence has shown that presenilin enhancer 2 (Pen2; Psenen) plays an essential role in corticogenesis by regulating the switch of apical progenitors (APs) to basal progenitors (BPs). The hippocampus is a brain structure required for advanced functions, including spatial navigation, learning and memory. However, it remains unknown whether Pen2 is important for hippocampal morphogenesis. To address this question, we generated *Pen2* conditional knockout (cKO) mice, in which Pen2 is inactivated in neural progenitor cells (NPCs) in the hippocampal primordium. We showed that *Pen2* cKO mice exhibited hippocampal malformation and decreased population of NPCs in the neuroepithelium of the hippocampus. We found that deletion of Pen2 neither affected the proliferative capability of APs nor the switch of APs to BPs in the hippocampus, and that it caused enhanced transition of APs to neurons. We demonstrated that expression of the Notch1 intracellular domain (N1ICD) significantly increased the population of NPCs in the *Pen2* cKO hippocampus. Collectively, this study uncovers a crucial role for Pen2 in the maintenance of NPCs during hippocampal development.

KEY WORDS: Pen2 (Psenen), Apical progenitor, Immature neuron, Basal progenitor, Hippocampus

INTRODUCTION

The hippocampus is a unique brain structure required for cognitive functions. It is well known that the hippocampus arises from the caudomedial edge of the dorsal telencephalic neuroepithelium adjacent to the cortical hem (CH). The hippocampus can be divided into three subdivisions, including the cornu ammonis (CA), the dentate gyrus (DG) and the fimbria (Altman and Bayer, 1990b,c). The hippocampus is known to play important roles in synaptic plasticity, learning and memory, and spatial navigation (Langston and Wood, 2009; Martin and Clark, 2007; Martin et al., 2000; Wood and Dudchenko, 2021). It is believed that 'place cells' in the hippocampus are crucial for spatial navigation in animals. For example, different place cells may fire at different locations and encode information in different tasks (Ainge et al., 2007; O'Keefe and Dostrovsky, 1971; Wood et al., 2000). Conversely, abnormalities in the hippocampus are associated with neurological disorders (Connor et al., 2004; Houser, 1990; Lurton et al., 1997; Tamminga et al., 2010; Walton et al., 2012).

Hippocampal morphogenesis involves a number of complex cellular processes, including formation of the hippocampal primordium, generation of neurons and glial cells in different subregions, and migration of neurons (Altman and Bayer, 1990a,b, c; Angevine, 1965). Whereas neural progenitor cells (NPCs) in the CA give rise to pyramidal neurons (Altman and Bayer, 1990c), those in the primary dentate matrix generate granule neurons, which migrate tangentially and ultimately populate in the DG (Altman and Bayer, 1990a). However, molecular mechanisms underlying hippocampal development are poorly understood.

Presenilin enhancer 2 (Pen2; Psenen) is the smallest subunit of the γ-secretase complex and exhibits multiple cellular functions. First, Pen2 is essential for proteolytic cleavage of presenilin proteins (PSs) (De Strooper, 2003). Second, Pen2 can act as a substrate- binding site for γ-secretase (Fukumori and Steiner, 2016; Shah et al., 2005). Third, Pen2 is essential for the endoproteolytic activity of γ-secretase (Bammens et al., 2011). Fourth, Pen2 can regulate apoptosis. For example, knockdown of Pen2 causes apoptotic cell death in zebrafish (Campbell et al., 2006). Finally, it has been shown that straight knockout (KO) of *Pen2* (*Psenen*) results in embryonic lethality (Bammens et al., 2011), and that conditional KO (cKO) of *Pen2* in telencephalic NPCs leads to postnatal lethality (Cheng et al., 2019). Thus, Pen2 is important for the survival of animals.

It has been reported that Pen2 is involved in the 19q13 microdeletion syndrome displaying microcephaly (Forzano et al., 2012; Gana et al., 2012), suggesting that Pen2 is important for the central nervous system (CNS). To study the role of Pen2 in cortical development, we previously took advantage of the *Emxl-Cre* mouse and generated cortical NPC-specific *Pen2* cKO mice (Cheng et al., 2019). The latter exhibit depletion of apical progenitors (APs) and a transiently increased number of basal progenitors (BPs) in the dorsal telencephalon (Cheng et al., 2019), suggesting that Pen2 may control the switch of APs to BPs in the developing cortex. However, it remains unknown what role Pen2 exerts during hippocampal morphogenesis.

To answer the above question, we employed the *hGfap-Cre* mouse, in which the expression of Cre is controlled by the human *Gfap* (glial fibrillary acidic protein) promoter (Brenner et al., 1994; Zhuo et al., 2001). It has been shown that Cre is widely expressed in pyramidal neurons in the CA and granule cells in the DG in the hippocampus of the *hGfap-Cre* mouse (Brenner et al., 1994; Zhuo et al., 2001). The crossing of *Pen2*$^{f/f}$ to *hGfap-Cre* allowed us to

[1]Ministry of Education (MOE) Key Laboratory of Model Animal for Disease Study, Model Animal Research Center, Jiangsu Key Laboratory of Molecular Medicine, Medical School, Nanjing University, 12 Xuefu Avenue, Nanjing, Jiangsu, China, 210061. [2]Department of Neurobiology, Key Laboratory of Human Functional Genomics of Jiangsu, Nanjing Medical University, Nanjing, Jiangsu, China, 211166. [3]Department of Anesthesiology, The Second Affiliated Hospital, Nanjing Medical University, Nanjing, China, 210003. [4]Co-innovation Center of Neuroregeneration, Nantong University, Nantong, China, 226001.

*Authors for correspondence (chenguiquan@nju.edu.cn, jimuhuo2019@126.com, gaojun@njmu.edu.cn)

M.-H.J., 0000-0003-4944-6436; G.C., 0000-0002-4674-5548

Handling Editor: François Guillemot
Received 18 October 2021; Accepted 4 May 2022

Development (2022) 149, dev200272. doi:10.1242/dev.200272

generate *Pen2* cKO mice, in which Pen2 is inactivated in NPCs in the developing hippocampus. We found that *Pen2* cKO mice exhibited hippocampal hypoplasia. We detected massive loss of APs in the *Pen2* cKO hippocampus. We observed decreased levels of Hes1 and Hes5, unchanged levels of neurogenin 2 (Ngn2) and increased levels of neurogenic differentiation1 (NeuroD1) in the *Pen2* cKO hippocampus. Together, this study highlights the importance of Pen2 in the developing hippocampus.

RESULTS

Hippocampal malformation in *Pen2* cKO mice

We aimed to investigate the physiological function of Pen2 in the developing hippocampus. To this end, floxed *Pen2* mice were crossed to *hGfap-Cre* to generate *Pen2* cKO (*Pen2$^{f/f}$;hGfap-Cre*) mice. To check the expression of Cre recombinase in the developing hippocampus, the *hGfap-Cre* mouse was bred with the *mTmG* reporter (Muzumdar et al., 2007) to obtain *hGfap-Cre;mTmG* (Fig. 1A). Co-staining experiments revealed abundant GFP$^+$/Pax6$^+$ cells in the hippocampal neuroepithelium in *hGfap-Cre;mTmG* mice at E13.5 (Fig. 1B). We found that GFP was distributed mainly in the cytoplasm and the processes of Pax6$^+$ cells (Fig. 1B). As Pax6 is a marker for APs, the above immunohistochemistry (IHC) results indicated that Cre is expressed in APs in the hippocampal neuroepithelium. Moreover, we performed co-staining of GFP/Tbr2. We observed numerous GFP$^+$/Tbr2$^+$ cells in *hGfap-Cre;mTmG* mice at E13.5 (Fig. 1B). Thus, Cre is also expressed in BPs in the developing hippocampus.

To compare Pen2 levels between control and *Pen2* cKO mice (Fig. 1C), western blotting was conducted using hippocampal lysates prepared from mice at postnatal day 0 (P0) (Fig. 1D). We observed a significant reduction of Pen2 in *Pen2* cKO mice compared with controls (Fig. 1D). Next, quantitative real-time PCR (qRT-PCR) was performed using RNA samples from hippocampi at E17.5. As expected, levels of *Pen2* mRNAs were significantly decreased in *Pen2* cKO embryos (Fig. 1E). The above results suggest efficient inactivation of Pen2 in the *Pen2* cKO hippocampus.

We next completed Nissl staining using brain sections from mice at P0 and P6 (Fig. 1F). We found that the hippocampus was small in *Pen2* cKO mice compared with littermate controls at different ages (Fig. 1F). Quantification results confirmed significant reductions in the average area of the *Pen2* cKO hippocampus at P0 and P6 (Fig. 1G). Thus, conditional deletion of Pen2 caused hippocampal malformation.

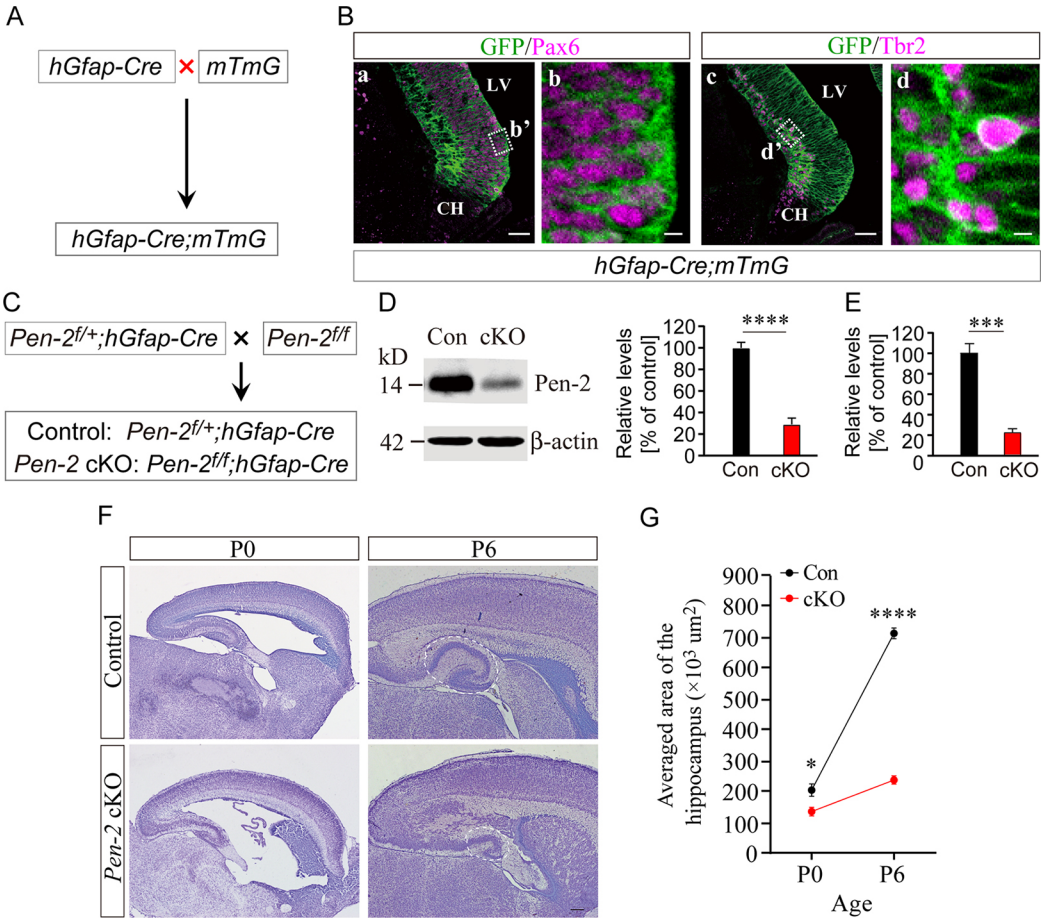

Fig. 1. Hippocampal malformation in *hGfap-Cre*-mediated *Pen2* cKO mice. (A) Breeding strategy for *hGfap-Cre;mTmG* mice. The *hGfap-Cre* mouse was crossed to the *mTmG*. (B) Representative images of co-staining for GFP and Pax6 (a,b) or Tbr2 (c,d) using *hGfap-Cre;mTmG* mice at E13.5. There was abundant colocalization for GFP/Pax6 (a,b) and GFP/Tbr2 (c,d) in the neuroepithelium in the hippocampal primordium. The boxed areas (b′ and d′) are enlarged in b and d, respectively. Scale bars: 50 µm for a,c; 5 µm for b,d. LV, lateral ventricle; CH, cortical hem. (C) Breeding strategy to generate *Pen2* cKO (*Pen2$^{f/f}$;hGfap-Cre*) mice. (D) Western blotting for Pen2. There was a highly significant difference in Pen2 protein levels between control and *Pen2* cKO mice at P0 (****P<0.001; n=5 mice per group). (E) Q-RT-PCR analysis of *Pen2* mRNAs. There was a highly significant difference in *Pen2* mRNA levels in the hippocampus between control mice and *Pen2* cKOs at E17.5 (***P<0.005; n=4 mice per group). (F) Nissl staining results. The hippocampus was smaller in *Pen2* cKO mice than in controls. Scale bar: 200 µm. (G) Average area of the hippocampus. There was a highly significant difference between control and *Pen2* cKO mice (for P0, *P<0.05; for P6, ****P<0.001; n=3 mice per group per age).

Development (2022) 149, dev200272. doi:10.1242/dev.200272

Loss of NPCs in the developing hippocampus of *Pen2* cKO mice

To explore cellular mechanisms underlying the above phenotype, we examined NPCs by conducting fluorescence immunohistochemistry on Pax6 and Tbr2 using brain sections at embryonic day 16.5 (E16.5) and E17.5. We found that the immunoreactivity of Pax6 in the hippocampal neuroepithelium was comparable between control and *Pen2* cKO mice at E16.5. Cell counting results revealed that the average number of Pax6$^+$ cells per section in the hippocampal neuroepithelium did not differ between control and *Pen2* cKO mice at E16.5 (Fig. 2C). In contrast, the immunoreactivity of Pax6 in the hippocampal neuroepithelium was decreased in *Pen2* cKO mice at E17.5 compared with littermate controls (Fig. 2A,B). In line with this, the number of Pax6$^+$ cells in the hippocampal neuroepithelium was less in *Pen2* cKO mice than in controls (Fig. 2C).

For results on BPs, the immunoreactivity of Tbr2 in the *Pen2* cKO hippocampus was comparable with that in controls at E16.5, and it was decreased in *Pen2* cKOs at E17.5 (Fig. 2D,E). The average number of Tbr2$^+$ cells in the hippocampus per section was unchanged in *Pen2* cKO mice at E16.5 compared with controls (Fig. 2F), and it was significantly decreased in *Pen2* cKOs at E17.5 (Fig. 2F).

We further studied whether NPCs were affected in the cortex of *Pen2* cKO mice. First, to examine the deletion efficiency of Pen2, we performed qRT-PCR analysis on *Pen2* using RNA samples from *Pen2* cKO cortices at E16.5, and we observed a significant reduction (Fig. S1A), suggesting that Pen2 is inactivated in the cortex. Second, the immunoreactivity of Pax6 in the cortex did not differ between control and *Pen2* cKO mice at E17.5 (Fig. S1B,C). We found that the average number of Pax6$^+$ cells per section was not significantly different between control and *Pen2* cKO mice (Fig. S1D). Third, we found that the immunoreactivity of Tbr2 in the cortex was comparable between control and *Pen2* cKO mice (Fig. S2A,B), and that there was no difference on the average number of Tbr2$^+$ cells between control and *Pen2* cKO mice (Fig. S2C). In addition, we performed immunohistochemistry using a number of markers for different cortical layers (Fig. S3). We observed that the immunoreactivity of Cux1, Ctip2 (Bcl11b) or Tbr1 did not differ between control and *Pen2* cKO mice at E17.5, and that the thickness of Cux1$^+$, Ctip2$^+$ or Tbr1$^+$ cell layers was comparable in these two genotypes (Fig. S3A-C). Thus, *hGfap-Cre*-mediated deletion of Pen2 did not cause significant effect on cortical lamination.

The neuroepithelium is the stem cell niche for APs/BPs in the hippocampal primordium, and it can be divided into the ammonic neuroepithelium (ANE) and the dentate neuroepithelium (DNE) [or the primary (1°) matrix] (Fig. 3A) (Altman and Bayer, 1990b; Galichet et al., 2008). The DNE gives rise to the secondary (2°) matrix and the tertiary (3°) matrix, and neurons in the CA or in the DG are generated from NPCs in the ANE or in the DNE, respectively (Tamminga et al., 2010). We counted Pax6$^+$ and Tbr2$^+$ cells at E17.5 for each subdivision separately. First, we found that the average number of Pax6$^+$ cells per section was significantly decreased in the ANE, the DNE and the 2° matrix in *Pen2* cKO mice at E17.5 compared with controls (Fig. 3B). There was no difference in the 3° matrix between control and *Pen2* cKO embryos (Fig. 3B). Second, the average number of Tbr2$^+$ cells in the ANE, the DNE and the 2° matrix, but not the 3° matrix, in control embryos significantly differed from that in *Pen2* cKO mice (Fig. 3C). Overall, these results confirmed the loss of NPCs by deletion of Pen2.

Unchanged proliferative capability of APs in the *Pen2* cKO hippocampus

To test the possibility that the depletion of APs in *Pen2* cKO mice may be due to deficient proliferation, we performed BrdU

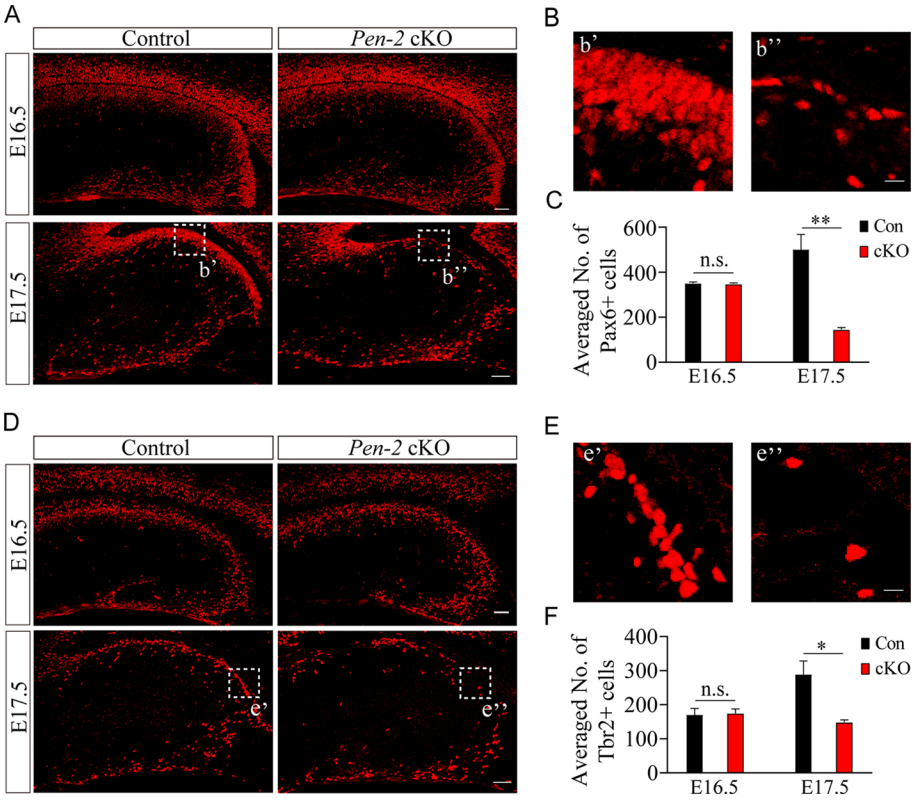

Fig. 2. Age-related loss of NPCs in the *Pen2* cKO hippocampus. (A) Representative images for immunohistochemistry of Pax6. Mice at E16.5 and E17.5 were used. (B) Enlarged images from the boxed areas in A. (C) Average number of Pax6$^+$ cells in the hippocampal neuroepithelium. There was a significant difference between control and *Pen2* cKO mice at E17.5 but not at E16.5 (**P<0.01; n.s., no significant; n=3 embryos per group per age). (D) Representative images for immunohistochemistry of Tbr2. Mice at E16.5 and E17.5 were examined. (E) Enlarged images from the boxed areas in D. (F) Average number of Tbr2$^+$ cells in the hippocampal neuroepithelium. There was significant difference between control and *Pen2* cKO mice at E17.5 but not at E16.5 (*P<0.05; n.s., no significant; n=3 embryos per group per age). Scale bars: 50 µm in A,D; 10 µm in B,E.

Development (2022) 149, dev200272. doi:10.1242/dev.200272

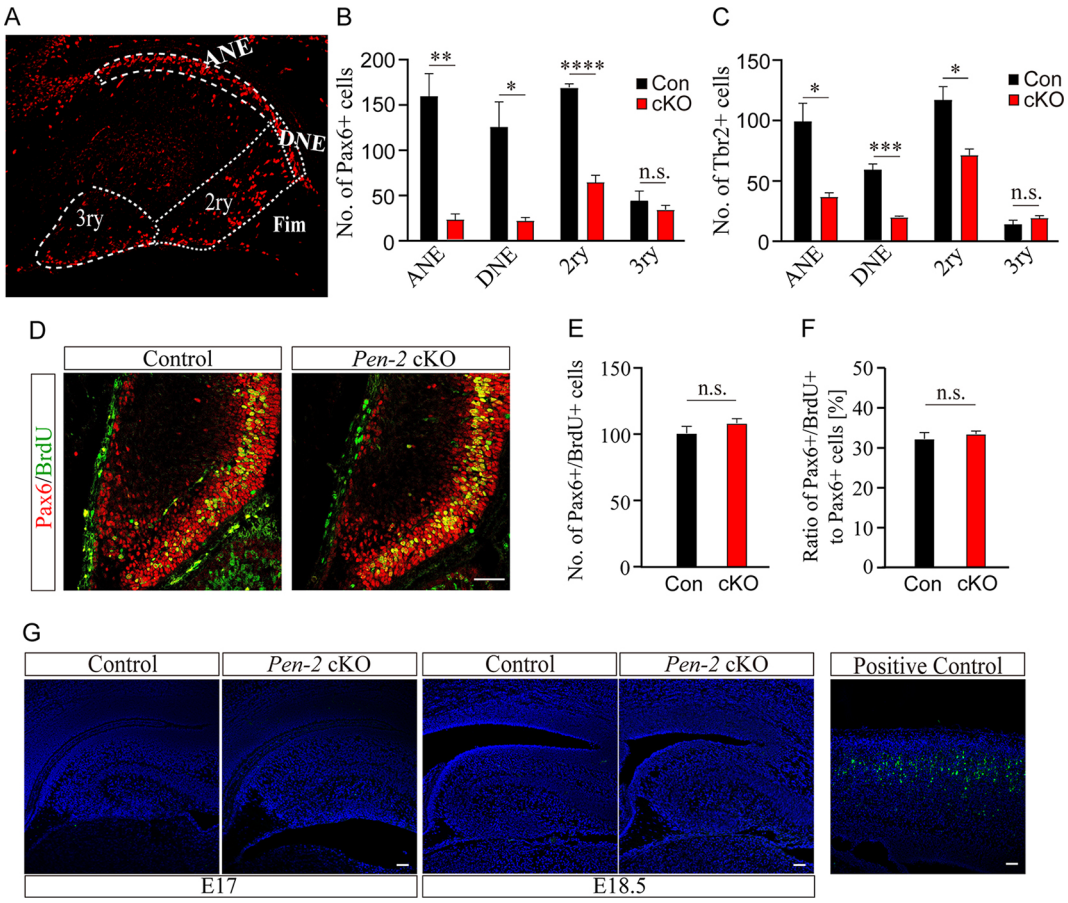

Fig. 3. Loss of NPCs in hippocampal subdivisions and unimpaired proliferative capacity of APs in the *Pen2* cKO hippocampus. (A) Four different subdivisions in the hippocampus are outlined, including the ANE, the DNE (or primary matrix), the secondary (2ry) matrix and the tertiary (3ry) matrix. ANE, ammonic neuroepithelium; DNE, dentate neuroepithelium. (B) Average number of Pax6$^+$ cells in each subdivision of the hippocampus. There were significant differences in the ANE, the DNE and the secondary matrix between control and *Pen2* cKO mice at E17.5 (****P<0.001; **P<0.01, *P<0.05; n=3 embryos per group). (C) Average number of Tbr2$^+$ cells in each subdivision in the hippocampus. There were significant differences in the ANE, the DNE and the secondary matrix between control and *Pen2* cKO mice at E17.5 (*P<0.05, ***P<0.005; n=3 embryos per group). (D) Representative images for co-staining of Pax6/BrdU in the hippocampus at E16.5. (E) Average number of Pax6$^+$/BrdU$^+$ in the hippocampal neuroepithelium at E16.5. There was no significant difference between control and *Pen2* cKO mice (n.s., no significant; n=3 embryos per group). (F) Ratio of the number of Pax6$^+$/BrdU$^+$ cells to the number of Pax6$^+$ cells in the hippocampal neuroepithelium at E16.5. There was no significant difference between control and *Pen2* cKO mice (n.s., no significant; n=3 embryos per group).
(G) Representative images for immunohistochemistry on cleaved caspase 3 (CC3) in the hippocampus at E17 and E18.5. No CC3$^+$ cells were detected in *Pen2* cKO mice compared with littermate controls. A brain section from *Ppp2ca* cKO mice at P0 was used as the positive control. Scale bars: 50 µm in D,G.

pulse-labeling experiments. BrdU was injected intraperitoneally to pregnant dams at E16.5 and embryos were collected 30 min after the injection. Double-staining experiments revealed no significant reduction on the total number of Pax6$^+$/BrdU$^+$ cells in the hippocampal neuroepithelium in *Pen2* cKO mice compared with controls (Fig. 3D,E). Moreover, the ratio of the number of Pax6$^+$/BrdU$^+$ cells to that of Pax6$^+$ cells did not differ between control and *Pen2* cKO mice at E16.5 (Fig. 3F). Thus, the ability to enter the synthesis phase (S-phase) of the cell cycle for *Pen2* cKO APs was not different from that for controls, suggesting unimpaired proliferation by deletion of Pen2. Hence, the depletion of APs in the *Pen2* cKO hippocampus was unlikely due to the proliferative capability of APs.

To test whether deletion of Pen2 affected apoptosis, we conducted immunohistochemistry on cleaved caspase 3 (CC3) using brains sections at E17 and E18.5 (Fig. 3G). We used NPC-specific *Ppp2cα* cKO mice as the positive control, as these mutants display robust apoptosis in the cortex (Huang et al., 2020). However, CC3$^+$ cells were not detected in control and *Pen2* cKO mice at E17 and E18.5 compared with *Ppp2cα* cKO mice (Fig. 3G). Thus, the loss of NPCs in *Pen2* cKO mice may not be due to abnormal cell death.

Enhanced transition of APs to neurons in the *Pen2* cKO hippocampus

We have recently shown that *Emx1-Cre*-mediated deletion of Pen2 causes transiently increased population of BPs in the telencephalon (Cheng et al., 2019). As the number of BPs in *Pen2* cKO hippocampi was unchanged at E16.5 but decreased at E17.5 (Fig. 2D-F), we then analyzed Tbr2$^+$ cells in mice at E17 (Fig. 4A). We found that the immunoreactivity of Tbr2 in the hippocampus was comparable between control and *Pen2* cKO mice (Fig. 4A). Moreover, the number of Tbr2$^+$ cells in the hippocampus was not significantly different between control and *Pen2* cKO mice (Fig. 4B). Overall, the results for Tbr2$^+$ cells at E16.5, E17 or E17.5 indicated no transient increase in BPs in the *Pen2* cKO hippocampus.

To study whether deletion of Pen2 affected the differentiation of APs into BPs in the hippocampus, we carried out double staining of Sox2/Tbr2 using brain sections at E17 (Fig. 4C). We found that the

Development (2022) 149, dev200272. doi:10.1242/dev.200272

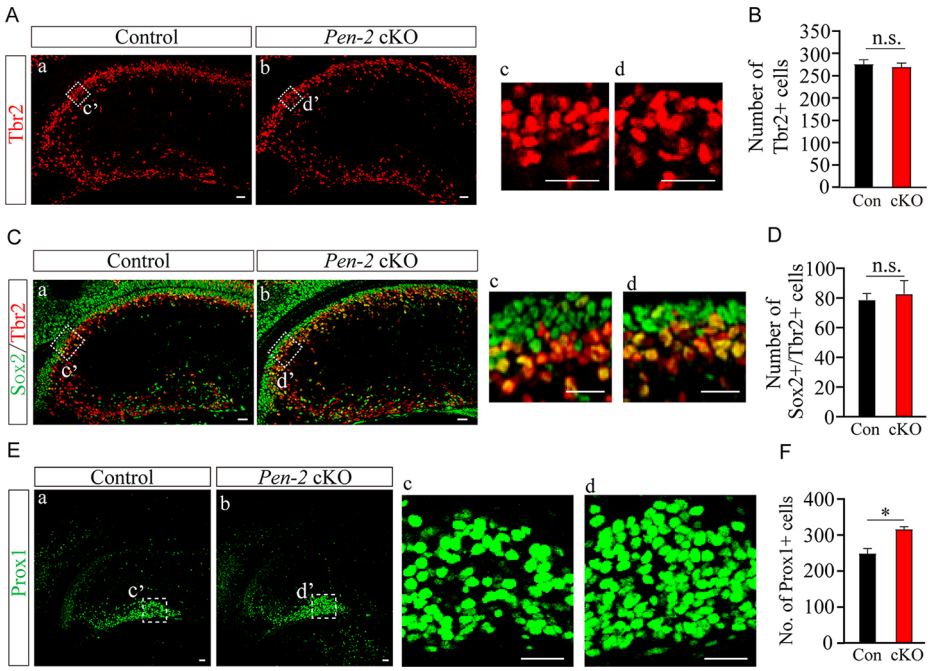

Fig. 4. Transiently increased numbers of neurons in the *Pen2* cKO hippocampus. (A) Representative images for immunohistochemistry for Tbr2 in the hippocampus at E17. The immuno-reactivity of Tbr2 was comparable between control and *Pen2* cKO mice (*n*=3 embryos per group). The boxed areas in a and b are enlarged in c and d, respectively. (B) Average number of Tbr2$^+$ cells in the hippocampus at E17. There was no significant difference between control and *Pen2* cKO mice (n.s., not significant; *n*=3 embryos per group). (C) Representative images for co-staining of Sox2/Tbr2 in the hippocampus at E17. The immunoreactivity of Tbr2 was comparable between control and *Pen2* cKO mice (*n*=3 embryos per group). The boxed areas in a and b are enlarged in c and d, respectively. (D) Average number of Sox2$^+$/Tbr2$^+$ cells in the hippocampus at E17. There was no significant difference between control and *Pen2* cKO embryos (*P*>0.7; *n*=3 embryos per group). (E) Representative images of immunohistochemistry for Prox1 in the hippocampus from mice at E17. There was increased immunoreactivity for Prox1 in *Pen2* cKO mice. The boxed areas in a and b are enlarged in c and d, respectively. (F) Average number of Prox1$^+$ cells in the hippocampus. There was significant difference between control and *Pen2* cKO mice at E17 (*P<0.05; *n*=3 embryos per group). Scale bars: 25 µm in A,C,E.

average number of Sox2$^+$/Tbr2$^+$ cells in the hippocampus did not differ between control and *Pen2* cKO mice (Fig. 4D), suggesting no significant change on BPs being differentiated from APs by deletion of Pen2. To study whether deletion of Pen2 altered neurogenesis, we examined neurons in the hippocampus at E17. Prox1, a marker for granule neurons, was used to perform immunohistochemistry (Fig. 4E). We observed significantly increased number of Prox1$^+$ cells in the hippocampus in *Pen2* cKO mice compared with littermate controls (Fig. 4F), suggesting transiently increased neurogenesis.

To test whether deletion of Pen2 affected the differentiation of APs into neurons in the hippocampus, we conducted double-staining for Pax6/NeuroD1 and Sox2/Tbr1 using brain sections at E17. We chose NeuroD1 and Tbr1 to label hippocampal neurons for the following reasons. First, hippocampal subregions, including the CA1, the CA3 and the DG were reduced in *Pen2* cKO mice at P2 or P6 (Fig. 1F), suggesting that both granule neurons and pyramidal neurons may be affected. Second, it has been shown that NeuroD1 is expressed in immature granule cells in the hippocampus (Nakahira and Yuasa, 2005; Pleasure et al., 2000). Third, it has previously been reported that Tbr1 may label both granule cells (in the CA3 and the DG) and pyramidal cells (in the CA1) in the developing hippocampus at E14, E16 and E18 (Barry et al., 2008).

We found that the immunoreactivity of NeuroD1 (Fig. 5A,B) was increased in the *Pen2* cKO hippocampus at E17 compared with controls (control=100%±4.1%, cKO=131%±1.7%; P<0.01). Next, we counted cells doubly positive for Pax6 and NeuroD1. We observed a significantly increased number of Pax6$^+$/NeuroD1$^+$ cells in the hippocampal neuroepithelium in *Pen2* cKO mice compared with controls (Fig. 5C). As NeuroD1 is crucial for the differentiation of granule cells in the hippocampus (Miyata et al., 1999), we further analyzed the immunoreactivity of NeuroD1 in the hippocampal neuroepithelium, and it was significantly increased in the *Pen2* cKO group compared with the control (Fig. 5D).

For double-staining of Sox2/Tbr1 (Fig. 5E,F), there was increased immunoreactivity of Tbr1 in the *Pen2* cKO hippocampus at E17 compared with littermate controls (control=100%±2%, cKO=126.5% ±3.1%; P<0.01). Sox2$^+$/Tbr1$^+$ cells in the hippocampal neuroepithelium were counted, and the number was highly increased in *Pen2* cKO mice (Fig. 5G). Overall, the above results suggest that loss of Pen2 may cause enhanced transition of APs to neurons in the hippocampus.

Deficient Notch signaling in the *Pen2* cKO hippocampus

To explore molecular mechanisms underlying the malformation of the *Pen2* cKO hippocampus, we analyzed several downstream targets of γ-secretase. Western blotting was conducted using protein samples from hippocampi at P0. We found that levels of the C-terminal fragment of PS1 (PS1-CTF) were decreased in *Pen2* cKO mice compared with controls (Fig. 6A). We observed a significant increase in the levels of the C-terminal fragment of amyloid precursor protein (APP-CTF) in *Pen2* cKO mice (Fig. 6A). The above results were in agreement with the notion that Pen2 is an essential component of the γ-secretase complex (De Strooper, 2003).

We next used total RNA samples prepared from the hippocampus at E17.5 to carry out qRT-PCR analyses on *Hes1* and *Hes5*, two key members in the Notch signaling. We found that mRNA levels for

Development (2022) 149, dev200272. doi:10.1242/dev.200272

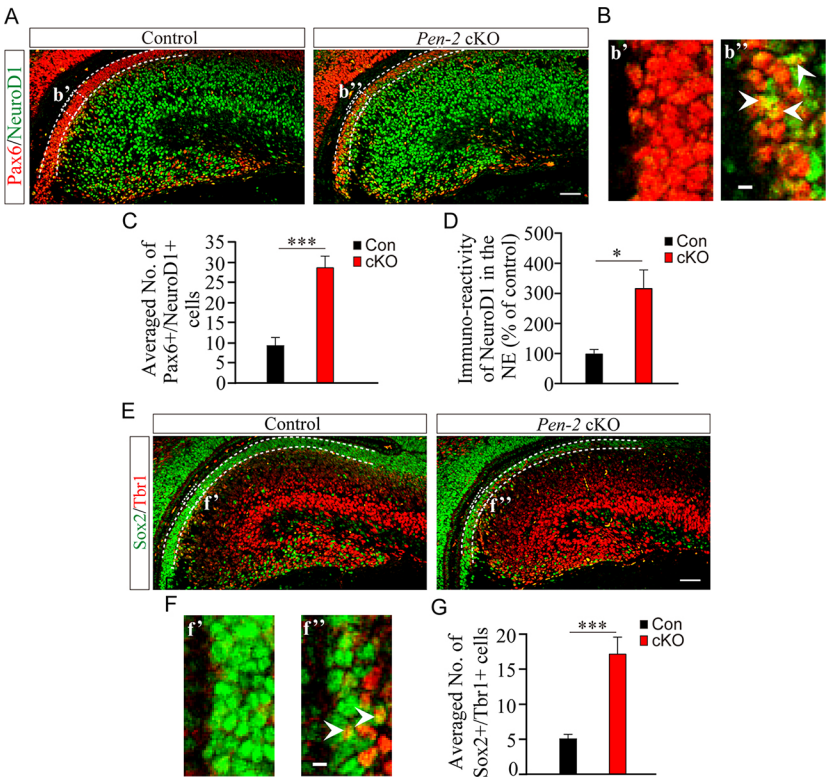

Fig. 5. Enhanced transition of APs to neurons in the *Pen2* cKO hippocampus. (A) Representative images of double staining for Pax6/NeuroD1 using brain sections at E17. The hippocampal neuroepithelium is outlined by two dashed lines. (B) Enlarged images from the boxed areas in A. Positive cells are indicated by white arrowheads. (C) Average number of $Pax6^+/NeuroD1^+$ cells in the hippocampal ventricular zone at E17. There was significant difference between control and *Pen2* cKO embryos (***P<0.005; n=3 embryos per group). (D) The immunoreactivity of NeuroD1 in the *Pen2* cKO hippocampal neuroepithelium as a percentage of that in the control. There was significant difference between control and *Pen2* cKO embryos at E17 (*P<0.05; n=3 embryos per group). (E) Representative images for double-staining of Sox2/Tbr1 at E17. The hippocampal neuroepithelium is outlined by two dashed lines. (F) Enlarged images from the boxed areas in E. Positive cells are indicated by white arrowheads. (G) Average number of $Sox2^+/Tbr1^+$ cells in the hippocampal neuroepithelium at E17. There was significant difference between control and *Pen2* cKO embryos (***P<0.005; n=3 embryos per group). Scale bars: 50 µm in A,E 10 µm in B,F.

Hes1 and *Hes5* were significantly decreased in the *Pen2* cKO hippocampus compared with controls (Fig. 6B). Moreover, levels for *Hey1* and *Hey2* mRNAs were also significantly decreased in the *Pen2* cKO hippocampus compared with controls (Fig. 6B). These results thus confirmed impaired Notch signaling in *Pen2* cKO mice.

We have recently found that *Emx1-Cre*-mediated deletion of Pen2 leads to increased levels of neurogenin 2 (Ngn2), which may account for enhanced switch of APs to BPs in the dorsal telencephalon (Cheng et al., 2019). Surprisingly, we found that mRNA levels of *Ngn2* were unchanged in the hippocampus of *Pen2$^{f/f}$;hGfap-Cre* mice (Fig. 6C). It is likely that Ngn2 may not be involved in Pen2-dependent transition of APs to neurons in the hippocampus. In contrast, our qRT-PCR analysis revealed significantly increased mRNA levels of *Neurod1* in the *Pen2* cKO hippocampus (Fig. 6C), indicating upregulation of *Neurod1* expression. Additionally, we examined Prox1 and Tbr1, which are proneuronal transcriptional factors. However, mRNA levels for *Prox1* and *Tbr1* in the hippocampus did not differ between control and *Pen2* cKO mice at E17.5 (Fig. 6D). Thus, the transcription of *Prox1* or *Tbr1* was not affected by deletion of Pen2.

Given that *Pen2* cKO embryos exhibited loss of NPCs at E17.5 (Fig. 2), the change in APP cleavage products and Notch targets in the E17.5 hippocampus (Fig. 6A-C) could be a consequence of the decreased population of progenitors. To exclude this possibility, we examined major Notch targets in *Pen2* cKO mice at E16.5, an age when the loss of NPCs was not seen (Fig. 2). As the mouse hippocampus at E16.5 is very small, the resulting protein lysates are insufficient for us to run western blotting. Therefore, we dissected the E16.5 hippocampus to prepare RNA samples. We then conducted qRT-PCR analysis. First, our results revealed a remarkable reduction in *Pen2* mRNA levels in the hippocampus of *Pen2* cKO mice at E16.5 compared with controls (Fig. 6E). For *Pen2* cKO mice at E16.5, the reduction on *Pen2* mRNAs in the hippocampus (Fig. 6E) was greater than in the cortex (Fig. S1A), suggesting higher deletion efficiency of *Pen2* in the hippocampus. Second, we observed significantly decreased levels of *Hes1* and *Hes5* in *Pen2* cKO mice at E16.5 compared with controls (Fig. 6E). The above results suggest that *hGfap-Cre*- mediated deletion of Pen2 is efficient in the hippocampus. Overall, the significant reduction in expression levels of *Hes1* and *Hes5* in the *Pen2* cKO hippocampus at E16.5 strongly suggests that molecular changes in Notch downstream targets precede the occurrence of the NPC loss at E17.5. Third, our qRT-PCR results revealed significantly increased levels of *Neurod1* but not *Ngn2* in the *Pen2* cKO hippocampus at E16.5 (Fig. 6F), suggesting that increased expression of *Neurod1* but not *Ngn2* may take place before *Pen2* cKO mice exhibit massive NPC loss at E17.5. As NeuroD1 is an important proneuronal transcriptional factor (Imayoshi et al., 2008; Miyata et al., 1999), we reasoned that increased Neurod1 might drive the transition of APs to neurons in the *Pen2* cKO hippocampus.

Rescued populations of APs and BPs in the *Pen2* cKO hippocampus expressing Notch1 intracellular domain

The above molecular results suggest that the Notch signaling may be involved in Pen2-dependent transition of APs to neurons. To further test this hypothesis, we used a Tg line expressing the Notch1 intracellular domain (ICD) in a Cre-dependent manner (Cheng et al., 2019). This Tg mouse was bred with *Pen2$^{f/f}$* and *Pen2$^{f/+}$;hGfap-Cre* to generate *Pen2$^{f/f}$;hGfap-Cre;LSL-N1ICD* (*Pen2* cKO*;N1ICD*) mice (Fig. 7A). First, qRT-PCR analysis confirmed significant reductions in *Pen2* mRNA levels in the hippocampus of *Pen2* cKO mice with and without N1ICD expression compared with littermate controls at E17.5 (Fig. 7B). Second, we found that levels of N1ICD were significantly increased in the hippocampus in *Pen2* cKO mice expressing N1ICD compared with those without N1ICD expression (Fig. 7B).

To examine whether Cre-dependent expression of N1ICD affected NPCs in *Pen2* cKO mice, brain sections at E17.5 were used for

Development (2022) 149, dev200272. doi:10.1242/dev.200272

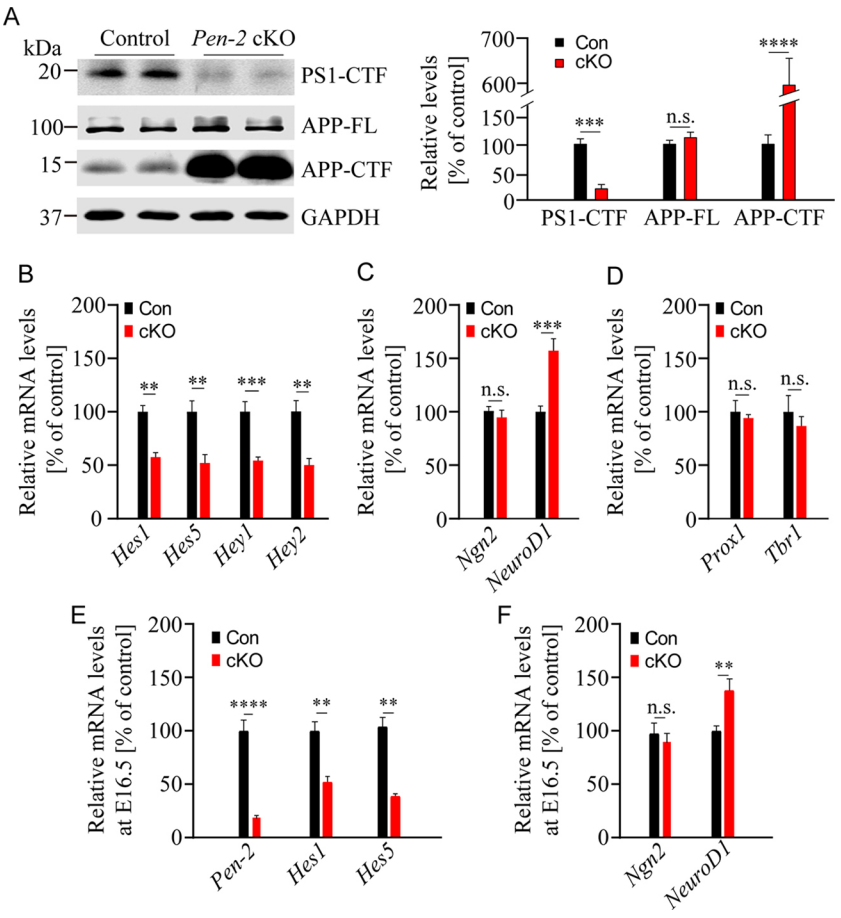

Fig. 6. Changes in γ-secretase downstream targets in the *Pen2* cKO hippocampus. (A) Western analyses of PS1-CTF, APP-FL and APP-CTF using hippocampal lysates at P0 (n=3 mice per group; ***P<0.005; ****P<0.001). (B) Q-RT-PCR analysis of members of the Notch signaling pathway. There was a significant difference in mRNA levels of *Hes1*, *Hes5, Hey1* and *Hey2* between control and *Pen2* cKO mice at E17.5 (n=4 mice per group; **P<0.01; ***P<0.005). (C) Q-RT-PCR analysis of the pro-neuronal transcriptional factors *Ngn2* and *Neurod1*. There was a significant difference in mRNA levels of *Neurod1* but not *Ngn2* between control and *Pen2* cKO mice at E17.5 (n=4 mice per group; n.s, not significant; ***P<0.005). (D) Q-RT-PCR analysis of *Prox1* and *Tbr1*. There was no significant difference in mRNA levels of *Prox1* or *Tbr1* between control and *Pen2* cKO mice at E17.5 (n=4 mice per group; n.s, not significant). (E,F) Q-RT-PCR analyses of *Pen2* and several downstream targets of γ-secretase in hippocampal RNA samples at E16.5. (E) There was a large decrease in levels of *Pen2* mRNA in *Pen2* cKO hippocampi at E16.5 (n=6 mice per group; ****P<0.001) and significant differences in the mRNA levels of *Hes1* and *Hes5* between control and *Pen2* cKO mice at E16.5 (n=4 mice per group; **P<0.01). (F) There was a significant difference in mRNA levels of *Neurod1* but not *Ngn2* between control and *Pen2* cKO mice at E16.5 (n=6 mice per group; n.s, not significant; **P<0.01).

immunohistochemistry on Pax6 and Tbr2 (Fig. 7C-F). Pax6$^+$ cells and Tbr2$^+$ cells in the hippocampal neuroepithelium were counted and then averaged. First, whereas Pax6$^+$ cells were hardly observed in the *Pen2* cKO hippocampus, they were abundantly present in control and in *Pen2* cKO mice expressing N1ICD (Fig. 7C). Quantification results revealed a significantly increased number of Pax6$^+$ cells in the hippocampal neuroepithelium in *Pen2* cKO mice expressing N1ICD compared with those without N1ICD expression (Fig. 7D). Second, we observed abundant Tbr2$^+$ cells in control and *Pen2* cKO mice expressing N1ICD (Fig. 7E). We found that there was a significantly increased number of Tbr2$^+$ cells in hippocampal neuroepithelium in *Pen2* cKO mice expressing N1ICD compared with those without N1ICD expression (Fig. 7F). Hence, Cre-dependent expression of N1ICD partially rescued populations of APs and BPs in the *Pen2* cKO hippocampus.

To examine whether the expression of N1ICD affected the population of neurons in *Pen2* cKO mice, we conducted IHC on Prox1 using brain sections at E17.5 (Fig. 8A). We counted Prox1$^+$ cells in the dentate migrating stream (DMS) and the DG. We found that there was a significantly decreased number of Prox1$^+$ cells in the DMS in *Pen2* cKO mice without N1ICD expression compared with those expressing N1ICD (Fig. 8B). Therefore, conditional expression of N1ICD rescued the neuronal population in the *Pen2* cKO hippocampus.

Increased expression of Hes1/Hes5 in the *Pen2* cKO hippocampus expressing Notch1 ICD

To examine whether Cre-dependent expression of N1ICD rescued the Notch signaling in *Pen2* cKO mice, we performed *in situ* hybridization on *Hes1* and *Hes5* using brain sections at E16.5. We observed very faint Hes1$^+$ and Hes5$^+$ signals in the hippocampal neuroepithelium of *Pen2* cKO mice. We found that Hes1$^+$ and Hes5$^+$ signals were comparable between control and *Pen2* cKO; *N1ICD* mice (Fig. 8C), suggesting enhanced Notch signaling by the expression of N1ICD in *Pen2* cKO mice.

We next performed *in vitro* experiments to examine the effect of N1ICD on Hes1/Hes5. HEK293T cells were transfected with a vector carrying the *N1ICD* element and one expressing a luciferase reporter driven by the promoter of *Hes1* or *Hes5*. We found that the expression of N1ICD significantly enhanced the promoter activity of *Hes1* or *Hes5* (Fig. 8D), suggesting that N1ICD may positively regulate the expression of *Hes1* or *Hes5*. We then constructed plasmids expressing Hes1/HA or Hes5/HA (Fig. 8E). HEK293T cells were then transfected with a vector carrying the *Hes1* or *Hes5* gene and with one expressing a luciferase reporter driven by the *Neurod1* promoter. We found that the expression of Hes1 or Hes5 significantly inhibited the promoter activity of *Neurod1* (Fig. 8F), suggesting that Hes1 or Hes5 may negatively regulate the expression of *Neurod1*. Moreover, we found that co-transfection using vectors expressing Hes1, Hes5 and the luciferase reporter for the *Neurod1* promoter also caused significantly decreased promoter activity of *Neurod1* in HEK293T cells (Fig. 8F). Together, the above *in vitro* data suggest that N1ICD may regulate the expression of *Neurod1* via Hes1 and Hes5.

DISCUSSION

Recent evidence has revealed the involvement of Pen2 in microcephaly related to the 19q13 microdeletion (Forzano et al.,

Development (2022) 149, dev200272. doi:10.1242/dev.200272

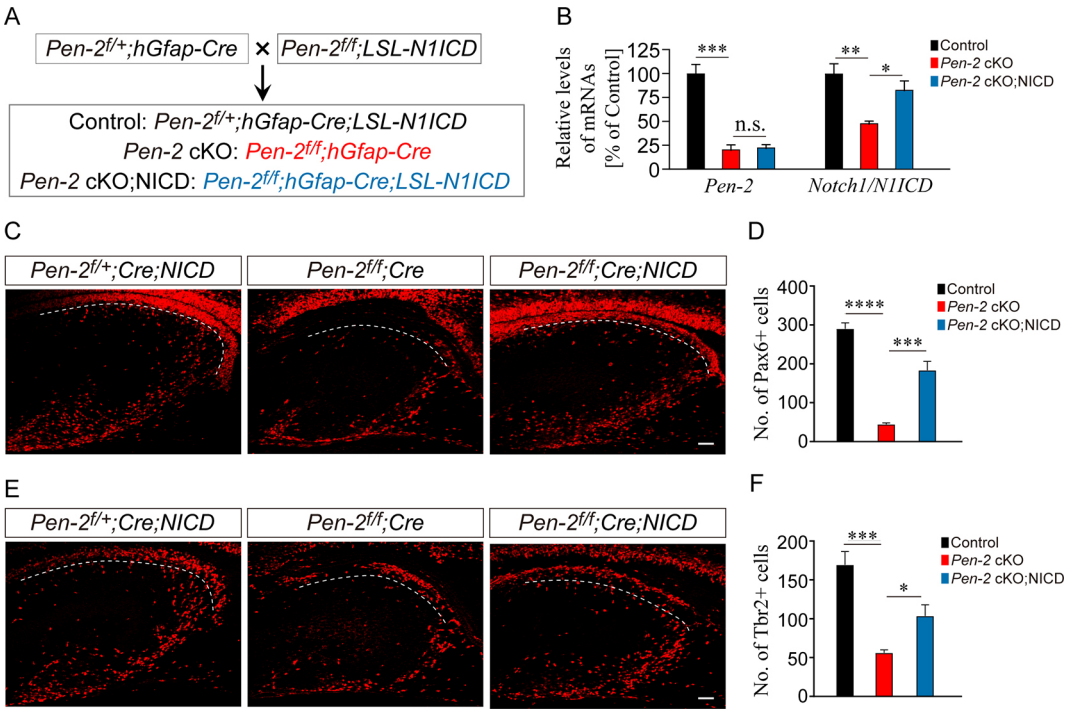

Fig. 7. Restored populations of NPCs and neurons in the *Pen2* cKO hippocampus by the expression of the Notch1 ICD. (A) The strategy to generate *Pen2* cKO; *N1ICD* mice. *Pen2*$^{f/+}$*;hGfap-Cre* mice were crossed to *Pen2*$^{f/f}$*;LSL-N1ICD*. *Pen2*$^{f/+}$*;hGfap-Cre;LSL-N1ICD* mice served as the control for *Pen2*$^{f/f}$*;hGfap-Cre* and *Pen2*$^{f/f}$*;hGfap-Cre;N1ICD*. (B) Q-RT-PCR analyses. There were significant differences in the levels of *Pen2* and *N1ICD* between control and *Pen2* cKO mice at E17.5 (*n*=4 mice per group; **P*<0.05; ***P*<0.01; ****P*<0.005). (C) Representative images for immunohistochemistry on Pax6 using brain sections at E17.5. The dashed lines indicate boundaries to outline the hippocampal neuroepithelium. (D) Average number of Pax6$^+$ cells in the hippocampus. There was significant main genotype effect among groups (*P*<0.0001). There was a significant difference between *Pen2* cKO and control or *Pen2* cKO;*N1ICD* (control, *n*=3; *Pen2* cKO, *n*=3; *Pen2* cKO;*N1ICD*, *n*=4) (****P*<0.005; *****P*<0.001). (E) Representative images of immunohistochemistry for Tbr2. (F) Average number of Tbr2$^+$ cells in the hippocampus. There was a significant main genotype effect among groups (*P*<0.005). There was a significant difference between *Pen2* cKO and control or *Pen2* cKO;*N1ICD* (**P*<0.05; ****P*<0.005). Scale bars: 50 µm in C and E.

2012; Gana et al., 2012). We aim to investigate how Pen2 may regulate hippocampal growth. As straight knockout of Pen2 causes an embryonic lethal effect in mice, conditional KO techniques have been used to produce viable cell type-specific *Pen2* cKO mice for postnatal studies (Bi et al., 2021; Cheng et al., 2019; Hou et al., 2021). Here, we have generated a unique mouse model in which Pen2 is inactivated in NPCs in the hippocampal primordium. Our lineage-tracing experiments confirmed the expression of Cre in APs and BPs in the *Pen2* cKO hippocampus, which is in line with previous findings (Brenner et al., 1994; Zhuo et al., 2001). Importantly, the observation of abnormal hippocampus in *Pen2* cKO mice strongly suggests that Pen2 is required for hippocampal morphogenesis.

It is believed that AP may undergo one of three distinct fates during early stage of the CNS development (Imayoshi and Kageyama, 2014). For example, one AP can generate two daughter APs through symmetric division. Alternatively, one AP may produce one AP and one BP or neuron through asymmetric division (Imayoshi and Kageyama, 2014). One of the most significant findings in this study is the abundance of Sox2$^+$/Tbr1$^+$ cells and Pax6$^+$/NeuroD1$^+$ cells in the *Pen2* cKO hippocampus. Since these two types of cells represent immature neurons that are being differentiated from APs, the robust increase in them strongly suggests that deletion of Pen2 causes significantly enhanced transition of APs to neurons. In contrast, our BrdU pulse-labeling experiments revealed no significant change in the ratio of the number of Pax6$^+$/BrdU$^+$ cells to that of Pax6$^+$ cells in the hippocampus in *Pen2* cKO embryos. Therefore, deletion of Pen2 does not impair the proliferation of APs. In addition, we observed no significant change in the number of CC3$^+$ cells in the *Pen2* cKO hippocampus. Thus, deletion of Pen2 does not significantly promote cell death. These findings prompt us to exclude the possibility that the loss of APs in the hippocampus of *Pen2* cKO mice may be due to abnormal cell cycle or cell death.

In this study, we did not observe any significant increase in the population of Tbr2$^+$ cells in the *Pen2* cKO hippocampus at any age examined, e.g. E16.5, E17 or E17.5, suggesting that the generation of BPs is not significantly enhanced by deletion of Pen2. Moreover, there was no increase in the number of Sox2$^+$/Tbr2$^+$ cells in the *Pen2* cKO hippocampus, suggesting that the AP-to-BP switch is not promoted by deletion of Pen2. Given that there was an increased number of Prox1$^+$ cells and Sox2$^+$/Tbr1$^+$ cells in the *Pen2* cKO hippocampus at E17, we reason that Pen2 might regulate hippocampal growth by inhibiting the transition of APs into neurons but not into BPs. Interestingly, we have recently reported premature generation of BPs in the ventricular zone (VZ) in the *Pen2*$^{f/f}$*;Emx1-Cre* cortex (Cheng et al., 2019). Different timings for Pen2 deletion may account for distinct phenotypes in *Pen2*$^{f/f}$*;Emx1-Cre* and *Pen2*$^{f/f}$*;hGfap-Cre* mice. More specifically, *Emx1-Cre*-mediated deletion of *Pen2* causes increased transition of APs to BPs in the VZ of the telencephalon at E12.5 and E13.5 (Cheng et al., 2019). Whereas *hGfap-Cre*-mediated deletion of *Pen2* results in enhanced transition of APs to neurons in the hippocampal neuroepithelium at E17, it does not affect populations of APs and BPs in the cortex. The above discrepancy may be due to the following reasons. First, the starting time for Cre expression driven by the human *Gfap* promoter is later than that by the *Emx1* promoter

Development (2022) 149, dev200272. doi:10.1242/dev.200272

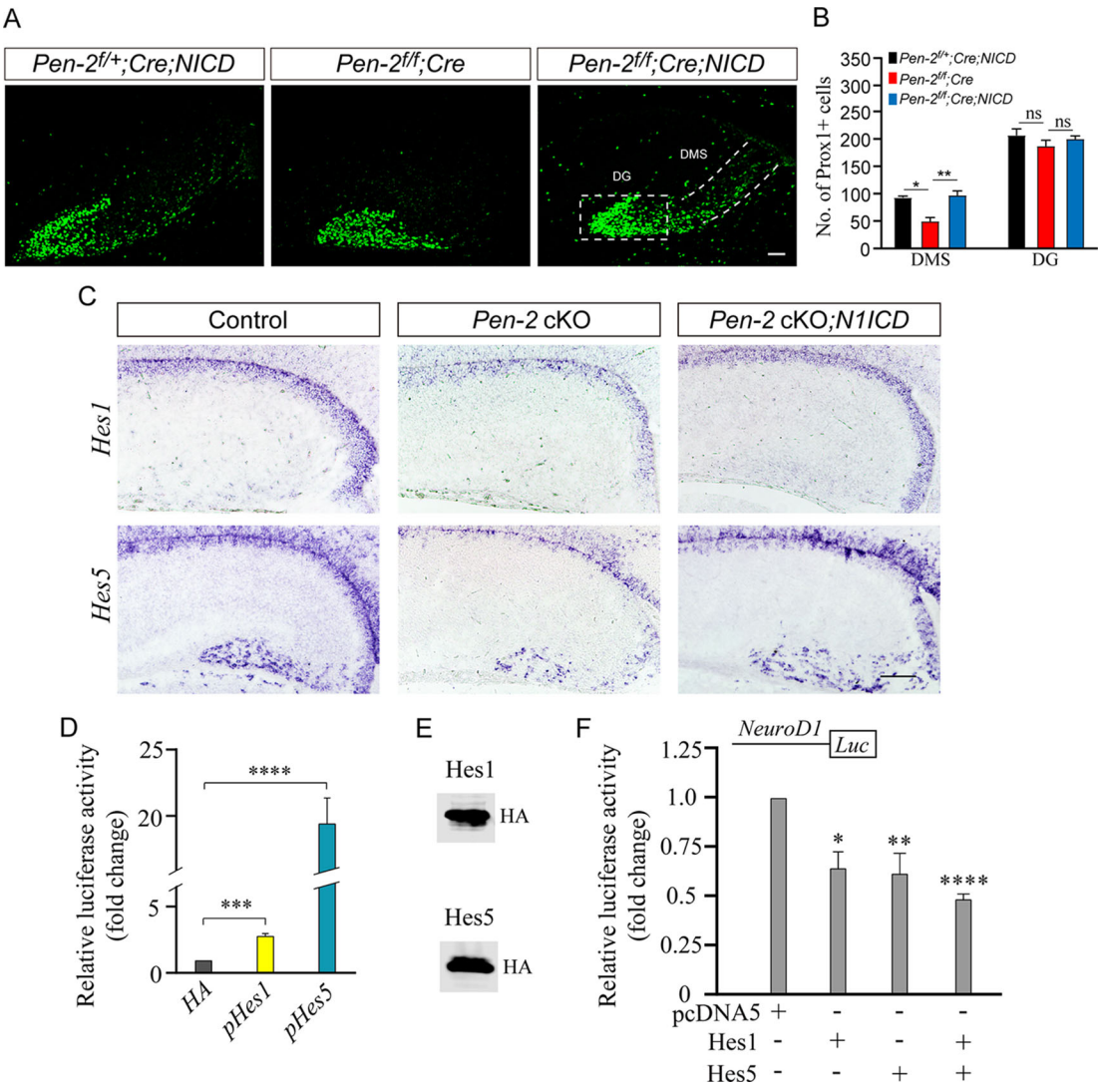

Fig. 8. Rescued expression of Hes1, Hes5 and Neurod1 by the expression of the Notch1 ICD in the *Pen2* cKO hippocampus. (A) Representative images of immunohistochemistry for Prox1 using brain sections at E17.5. (B) Average number of Prox1$^+$ cells in the DG and the DMS at E17.5 per section. There were significant differences between *Pen2* cKO and *Pen2* cKO;*N1ICD* mice (*P<0.05; **P<0.01). (C) *In situ* hybridization for *Hes1* and *Hes5*. Brain sections at E16.5 were used. Hes1$^+$ and Hes5$^+$ signals in the hippocampal neuroepithelium were increased in *Pen2* cKO;*N1ICD* mice compared with *Pen2* cKOs. (D) Luciferase assays on promoter activities for *Hes1* and *Hes5*. 293T cells were transfected with a vector carrying a luciferase reporter driven by the promoter of *Hes1* or *Hes5* together with one expressing N1ICD. Luciferase activities were measured 24 h after the transfection. Data are mean±s.e.m. There was a significant difference in relative luciferase activity between the HA group and the Hes1 or Hes5 group (***P<0.005; ****P<0.001; n=3 independent experiments). (E) Immunoblotting for HA. Plasmids expressing Hes1-HA or Hes5-HA were constructed. Western blotting confirmed the expression of HA in each plasmid. (F) Luciferase assays on promoter activities for *Neurod1*. 293 T cells were transfected with a vector carrying a luciferase reporter driven by the promoter of *Neurod1* together with one expressing pcDNA5-HA, Hes1, Hes5 or Hes1/Hes5. Data are mean±s.e.m. There were significant differences in relative luciferase activities between the pcDNA5 and the Hes1, the Hes5 and the Hes1/Hes5 groups (*P<0.05; **P<0.01; ****P<0.001; n=3 independent experiments). Scale bars: 50 µm in A; 200 µm in C.

(E13.5 versus E10.5). Second, *hGfap-Cre*-mediated deletion efficiency of Pen2 is higher in the hippocampus than in the cortex. Third, deletion efficiency of Pen2 in the cortex is lower in *Pen2$^{f/f}$;hGfap-Cre* mice than in *Pen2$^{f/f}$;Emx1-Cre* mice.

To identify molecular mechanisms underlying Pen2-dependent hippocampal growth, we have focused on the Notch signaling, a major downstream target of γ-secretase. As expected, mRNA levels of *Hes1*, *Hes5*, *Hey1* and *Hey2* are decreased by deletion of Pen2. Furthermore, the generation of *Pen2* cKO mice expressing N1ICD allowed us to observe a significant rescue effect on the population of APs in the hippocampus. Therefore, the Notch signaling may play a crucial role in Pen2-dependent fate determination of APs in the developing hippocampus. Interestingly, roles of Notch1, Rbpjκ or jagged 1 in the postnatal hippocampus (Breunig et al., 2007; Ehm et al., 2010; Lavado and Oliver, 2014) and the adult brain (Ables et al., 2011; Blackwood, 2019; Blackwood et al., 2020) have been studied by several groups. It has been shown that Notch1 may regulate the cell cycle exit of NPCs in the postnatal hippocampus (Breunig et al., 2007), and that jagged 1 regulates the proliferation of NPCs in the postnatal DG (Lavado and Oliver, 2014).

The following evidence indicates upregulation of NeuroD1, but not Ngn2, by deletion of Pen2 in the hippocampus. First, mRNA levels of *Neurod1*, but not *Ngn2*, were increased in *Pen2* cKO hippocampal lysates. Second, the immunoreactivity of NeuroD1 in the hippocampus was stronger in *Pen2* cKO mice than in controls.

Development (2022) 149, dev200272. doi:10.1242/dev.200272

Third, whereas the promoter activity of *Hes1* or *Hes5* was enhanced by N1ICD, that of *Neurod1* was repressed by Hes1 or Hes5. We reason that NeuroD1, but not Ngn2, may serve as the key molecular mechanism for enhanced transition of APs to neurons in the *Pen2* cKO hippocampus. Overall, the above findings are in agreement with the concept that NeuroD1 is important for cell fate specification (Guillemot, 2007). Indeed, it has been shown that straight knockout of NeuroD1 impairs neuronal differentiation (Liu et al., 2000b; Schwab et al., 2000), and that NeuroD1 is required for neuronal differentiation in different brain regions (Liu et al., 2000a; Miyata et al., 1999; Morrow et al., 1999).

As shown in Fig. 9, we propose a cellular model to summarize molecular mechanisms for Pen2-dependent maintenance of NPCs during hippocampal development. First, deletion of Pen2 in hippocampal APs causes loss of γ-secretase activity (Fig. 9). Second, the generation of NICD is prevented, followed by inhibition on the expression of Hes1/5 and other Notch targets (Fig. 9). Third, decreased Hes1/5 causes increased levels of NeuroD1, which may significantly enhance the transition of APs to neurons in the hippocampal neuroepithelium (Fig. 9). Fourth, populations of APs and BPs are subsequently decreased in various hippocampal subregions. It is worth mentioning that the pool of NPCs in the 3° matrix was unchanged in the *Pen2* cKO hippocampus at E17.5, suggesting that the number of DG-born neurons may be comparable between two genotypes. As neurons in the DG are generated from NPCs in the 3° matrix, as well as the DNE in the hippocampus (Nakahira and Yuasa, 2005), the reduction in NPC populations in the DNE in *Pen2* cKO mice at E17.5 suggests that the number of DNE-born neurons may be significantly decreased in *Pen2* cKO mice at and after E17.5. Overall, depletion of NPCs in the *Pen2* cKO hippocampal neuroepithelium may result in deficient neurogenesis in hippocampal subregions and consequently lead to hippocampal malformation.

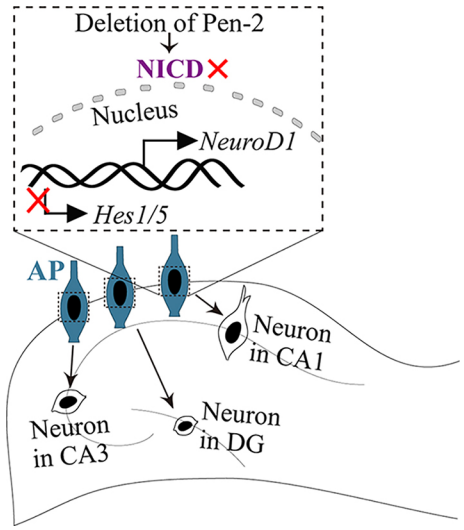

Fig. 9. Schematic model for the fate determination of APs regulated by Pen2. This model depicts molecular events involved in Pen2-dependent fate determination of APs. In *Pen2* cKO mice, γ-secretase activity is impaired so that Notch receptors cannot be cleaved to produce NICD. Inhibition of Notch causes downregulation of Hes1 and Hes5, which leads to increased expression of NeuroD1 in the hippocampus. NeuroD1 drives premature neuronal differentiation in the hippocampal neuroepithelium. Populations of APs and BPs are subsequently decreased in various hippocampal subregions. Finally, depletion of NPCs may cause deficient neurogenesis, which results in hippocampal malformation.

MATERIALS AND METHODS

Ethics statement

Mouse breeding was conducted under an Animal Protocol approved by the IACUC of the Model Animal Research Center (MARC) at Nanjing University. All mouse experiments were performed in accordance with the Guide for the Care and Use of Laboratory Animals of the MARC at Nanjing University.

Animals

Pen2$^{f/f}$, *LSL-N1ICD* and *mTmG* mice were reported by us recently (Bi et al., 2021; Cheng et al., 2019; Hou et al., 2021; Wang et al., 2021a). Human *Gfap-Cre* (Brenner et al., 1994) mice were purchased from the Jackson Laboratory. To generate *Pen2* cKO mice, we bred *Pen2$^{f/f}$* with *hGfap-Cre* to obtain *Pen2$^{f/+}$;hGfap-Cre*. The latter were crossed to *Pen2$^{f/f}$* to generate *Pen2$^{f/+}$;hGfap-Cre* (control) and *Pen2$^{f/f}$;hGfap-Cre* (*Pen2* cKO) mice. To generate *Pen2* cKO mice expressing N1ICD, we bred *Pen2$^{f/f}$* with *LSL-N1ICD* to produce *Pen2$^{f/+}$;LSL-N1ICD*, which were bred with *Pen2$^{f/f}$* to create *Pen2$^{f/f}$;LSL-N1ICD*. The latter were crossed to *Pen2$^{f/+}$;hGfap-Cre* to generate *Pen2$^{f/+}$;hGfap-Cre;LSL-N1ICD* (control) and *Pen2$^{f/f}$;hGfap-Cre;LSL-N1ICD* (*Pen2* cKO;*NICD*) mice. Genetic background of the mice used in this study was C57BL/6.

The mice were maintained in a SPF room in the core animal facility in the MARC at Nanjing University. Both male and female mice were used in this study. The mice were housed in groups (four to six mice per cage) and had *ad libitum* access to food and water. The animal room was maintained on a 12 h light/dark cycle. Lights were automatically turned on at 07:00 and switched off at 19:00. The room temperature was kept at 25±1°C. The birth date of the mice was defined as P0, and the day of vaginal plug detection in pregnant mice was E0.5.

Nissl staining

After neonatal mice were sacrificed, brains were dissected and then fixed in 4% paraformaldehyde (PFA) at 4°C overnight. Tissues were dehydrated with graded ethanol. After being embedded in paraffin, each block was sectioned sagittally using a microtome (the thickness of each was 10 µm). Each paraffin block contained four brains, including two control and two *Pen2* cKO littermates. Sections were deparaffinized with xylene and then treated with 0.1% Cresyl Violet for 2 min, followed by rinsing with distilled water for 1 min. Sections were air-dried and then sealed using neutral resin (Sinopharm Chemical Reagent). For each brain, a total of three sections spaced by 200 µm were used for measurement.

Immunohistochemistry

Pregnant mice were sacrificed with CO_2. Embryos were dissected out and then fixed in 4% PFA at 4°C overnight. Tissues were dehydrated using graded ethanol. Brains were embedded with paraffin. Each paraffin block contained one brain and was sectioned coronally using a microtome (10 µm in thickness). Sections were deparaffinized with xylene and then rehydrated with graded ethanol. Sections were boiled in sodium citrate buffer (0.01 M) for 25 min followed by blocking with 5% BSA at room temperature for 30 min. Sections were incubated with the primary antibody at 4°C overnight. For fluorescence immunohistochemistry, sections were incubated with the secondary antibody such as Alexa Fluor 488 goat anti-mouse (Jackson ImmunoResearch, 115-545-003, 1:500), Alexa Fluor 594 goat anti-rabbit (Jackson ImmunoResearch, 111-585-003, 1:500), Alexa Fluor Cy3 donkey anti-rabbit (Jackson ImmunoResearch, 711-165-152, 1:500), Alexa Fluor Cy5 donkey anti-goat (Jackson ImmunoResearch, 715-175-147, 1:500) or Alexa Fluor 488 donkey anti-rat (Abcam, ab150153, 1:500). Primary antibodies used for immunohistochemistry are listed in Table S1. Fluorescence images were captured using a TCS SP5 laser confocal microscope (Leica Microsystems) or a LSM880 laser confocal microscope (Zeiss).

Western blotting

Cortical and hippocampal samples were collected from newborn mice and embryos. Methods for western blotting have been described previously (Liu et al., 2017). Antibodies used for western blotting are listed in Table S1.

Development (2022) 149, dev200272. doi:10.1242/dev.200272

BrdU labeling

To label NPCs in proliferation, BrdU was intraperitoneally injected into pregnant mice (B5002, Sigma Aldrich; 100 mg/kg) and embryos were collected 30 min after the injection.

Cell counting

For quantification studies, three or four embryos in each genotype were used. For each embryo, at least two coronal sections spaced 100 µm apart were used for cell counting purposes. Fluorescence images for $Pax6^+$, $Tbr2^+$, $Pax6^+/BrdU^+$, $Pax6^+/NeuroD1^+$, $Sox2^+/Tbr1^+$, $Sox2^+/Tbr2^+$ and $Prox1^+$ cells were captured under the 20× objective lens of a TCS SP5 microscope. To count cells positive for Pax6 or Tbr2 in the hippocampus, the ANE, the DNE, the 2ry matrix and the 3ry matrix were outlined in images captured from each brain section, and cells were counted for each sub-region separately (Fig. 3B,C). In Figs 2C,F, 3E,F, 4B and 7D,F, the total number of positive cells in the hippocampus was the sum of cells in four different subregions. For results in Figs 4D and 5C,G, positive cells in the hipppocampal neuroepithelium were counted. Adobe Photoshop was used to count different types of cells. The experimenter was blind to genotypes of brain sections.

Measurement of immuno-reactivity

All the florescence images captured by Leica confocal microscope were converted to 8-bit images and the scale was set in pixels in ImageJ. The neuroepithelium in each section was manually outlined using the freehand selection tool in ImageJ. The immunoreactivity was defined as Raw Signal Intensity divided by the Area. Two sections spaced at 100 µm from each embryo were used for image capture and two images were used for measurement on the immunoreactivity for each embryo.

Quantitative real-time PCR

An ABI StepOne Plus machine was used for qRT-PCR. Total RNA (1µg) of each sample was reverse transcribed using the PrimeScript RT reagent Kit (Takara). RT-PCR was conducted using the 2× RealStar Green Fast Mixture with Rox (GenStar). All the primers used for qRT-PCR analyses were as follows; For *Pen2*, TGGATTTG CGTTCCTGCCTTTTCT (forward) and ATGAAGTTGTTAGGGAGTGCC (reverse); for *Hes1*, TCCAAGCTAG-AGAAGGCAGACA (forward) and CGCGGTATTTCCCC AACA (reverse); for *Hes5*, AACACAGCAAAGCCTTCGCC (forward) and AAGCA GCTTCATCTGCGTGTC (reverse); for *N1ICD*, ACTTGTCA-GATGTGGCCTCG (forward) and ATTCAAGTGGCTGATGCCCA (reverse); for *Hey1*, AGTTAACTCC TCCTTGCCCG (forward) and CGATGATGCCTCTCCGTCTT (reverse); for *Hey2*, GCTACAGGGGG-TAAAGGCTAC (forward) and GAGATGAGAGACAAGGCGCA (reverse); for *NeuroD1*, CAAAGCCACGGATCAATCTT (forward) and TCCCGGG AATAGTGAAACTG (reverse); for *Tbr1*, AGAGGCTCTGG-AAACACGAA (forward) and ACTCGACTCGCCTAGGAACA (reverse); for *Prox1*, CAGATGCAT TACCTCGCAGC (forward) and CTGGAACC-TCAAAGTCATTTGC (reverse); and for *GAPDH*, AATGTGTCCG-TCGTGGATCT (forward) and CCCTGTTGCTGTAGCCG TAT (reverse).

In situ hybridization

RNA isolation and reverse transcription are described in the qRT-PCR section. An 848 bp fragment of the *Hes1*-coding sequence (NM008235.2) was amplified by PCR using the following primers: ATGCCAGCTGA-TATAATGGA (forward) and TCAGTTCCGCCACGGTCTCC (reverse). A 902 bp fragment from the *Hes5* mRNA sequence (NM010419.4) was amplified by PCR using the following primers: AGGACTACAGCG-AGGGCTACTC (forward) and TTAGAA GCCTTCAGAACAGCCT (reverse). RNA probe labeled by digoxigenin (DIG) were prepared using the DIG RNA labeling kit (Roche, 11175025910) and purified using a RNA clean-up kit (Bioteck RP1801).

Brains were fixed in 4% PFA/DEPC-H_2O overnight and dehydrated in 30% sucrose/DEPC-PBS at 4°C overnight. Brains were embedded in OCT, then frozen quickly with liquid nitrogen. Coronal sections (12 µm) were prepared using a Leica CM 1950 cryostat at −20°C and stored at −80°C until use. After being incubated with the *Hes1* or *Hes5* probe at 65°C for 12 h, sections were washed and incubated with anti-DIG-AP Fab fragments (Roche, 11093274910) at room temperature for 3 h. The AP activity was developed using NBT/BCIP substrates (Roche).

Constructs of plasmids

Mouse *Hes1* and *Hes5* were constructed using the pcDNA5-HA vector (Hou et al., 2021; Wang et al., 2021a). The *Hes1*- and *Hes5*-coding sequences were amplified by PCR from cDNA libraries prepared from mouse brain. Plasmid expressing N1ICD was purchased from Addgene (Addgene, 20183). For the luciferase reporter assay, the promoter regions of *Hes1* (−2000 bp to 46 bp), *Hes5* (−1941 bp to 427 bp) or *Neurod1* (−2100 bp to 406 bp) were constructed using pGL3-Luc vector.

Luciferase reporter assay

293 T cells were cultured in DMEM supplemented with 10% FBS and 1% penicillin-streptomycin at 37°C in an incubator, and transfected by Lipofectamine-2000 (Invitrogen). The luciferase assay was performed using Dual-Glo (Promega) according to the manufacturer's protocol 24 h after the transfection. A CMV promoter-driven Renilla luciferase was used as the internal control. Data were obtained from at least three independent experiments.

Statistical analysis

Data are presented as mean±s.e.m. Owing to highly homogeneous phenotypes in *Pen2* cKO mice, the sample size of three or four for each genotype was used for cell counting according to recently published studies (Ahrendsen et al., 2018; Lavado et al., 2010; Liu et al., 2019; Wang et al., 2021b; Zou et al., 2014). GraphPad Prism7 and *t*-tests (two-tailed) were used for statistical analysis to examine main genotype effects between control and *Pen2* cKO groups. One-way ANOVA with multiple comparisons was conducted to evaluate genotype effects in experiments using mice with and without expression of N1ICD. $P<0.05$ is considered as statistically significant.

Acknowledgements

We thank Drs Tingting Liu, Jinxing Hou, He Wang and Shanshan Cheng for advice and technical assistance.

Competing interests

The authors declare no competing or financial interests.

Author contributions

Conceptualization: G.C.; Methodology: Y.X., Y.Z., M.X., X.Z.; Investigation: Y.X., Y.Z., M.X., X.Z.; Data curation: G.C., J.G., M.-H.J.; Supervision: G.C., M.-H.J., J.G.

Funding

This work was supported by grants from the National Natural Science Foundation of China (91849113 and 31271123) and the Natural Science Foundation of Jiangsu (BK20201255 and BK20191081).

Peer review history

The peer review history is available online at https://journals.biologists.com/dev/article-lookup/doi/10.1242/dev.200272

References

Ables, J. L., Breunig, J. J., Eisch, A. J. and Rakic, P. (2011). Not(ch) just development: Notch signalling in the adult brain. *Nat. Rev. Neurosci.* **12**, 269-283. doi:10.1038/nrn3024

Ahrendsen, J. T., Harlow, D. E., Finseth, L. T., Bourne, J. N., Hickey, S. P., Gould, E. A., Culp, C. M. and Macklin, W. B. (2018). The protein tyrosine phosphatase Shp2 regulates oligodendrocyte differentiation and early myelination and contributes to timely remyelination. *J. Neurosci.* **38**, 787-802. doi:10.1523/JNEUROSCI.2864-16.2017

Ainge, J. A., van der Meer, M. A. A., Langston, R. F. and Wood, E. R. (2007). Exploring the role of context-dependent hippocampal activity in spatial alternation behavior. *Hippocampus* **17**, 988-1002. doi:10.1002/hipo.20301

Altman, J. and Bayer, S. A. (1990a). Migration and distribution of two populations of hippocampal granule cell precursors during the perinatal and postnatal periods. *J. Comp. Neurol.* **301**, 365-381. doi:10.1002/cne.903010304

Altman, J. and Bayer, S. A. (1990b). Mosaic organization of the hippocampal neuroepithelium and the multiple germinal sources of dentate granule cells. *J. Comp. Neurol.* **301**, 325-342. doi:10.1002/cne.903010302

Altman, J. and Bayer, S. A. (1990c). Prolonged sojourn of developing pyramidal cells in the intermediate zone of the hippocampus and their settling in the stratum pyramidale. *J. Comp. Neurol.* **301**, 343-364. doi:10.1002/cne.903010303
Angevine, J. B., Jr. (1965). Time of neuron origin in the hippocampal region. An autoradiographic study in the mouse. *Exp. Neurol Suppl.* **2**, 1-70.
Bammens, L., Chavez-Gutierrez, L., Tolia, A., Zwijsen, A. and De Strooper, B. (2011). Functional and topological analysis of Pen-2, the fourth subunit of the gamma-secretase complex. *J. Biol. Chem.* **286**, 12271-12282. doi:10.1074/jbc.M110.216978
Barry, G., Piper, M., Lindwall, C., Moldrich, R., Mason, S., Little, E., Sarkar, A., Tole, S., Gronostajski, R. M. and Richards, L. J. (2008). Specific glial populations regulate hippocampal morphogenesis. *J. Neurosci.* **28**, 12328-12340. doi:10.1523/JNEUROSCI.4000-08.2008
Bi, H., Zhou, C., Zhang, Y., Cai, X., Ji, M., Yang, J., Chen, G. and Hu, Y. (2021). Neuron-specific deletion of presenilin enhancer2 causes progressive astrogliosis and age-related neurodegeneration in the cortex independent of the Notch signaling. *CNS Neurosci. Ther.* **27**, 174-185. doi:10.1111/cns.13454
Blackwood, C. A. (2019). Jagged1 is essential for radial glial maintenance in the cortical proliferative zone. *Neuroscience* **413**, 230-238. doi:10.1016/j.neuroscience.2019.05.062
Blackwood, C. A., Bailetti, A., Nandi, S., Gridley, T. and Hebert, J. M. (2020). Notch dosage: Jagged1 haploinsufficiency is associated with reduced neuronal division and disruption of periglomerular interneurons in mice. *Front. Cell Dev. Biol.* **8**, 113. doi:10.3389/fcell.2020.00113
Brenner, M., Kisseberth, W. C., Su, Y., Besnard, F. and Messing, A. (1994). Gfap promoter directs astrocyte-specific expression in transgenic mice. *J. Neurosci.* **14**, 1030-1037. doi:10.1523/JNEUROSCI.14-03-01030.1994
Breunig, J. J., Silbereis, J., Vaccarino, F. M., Sestan, N. and Rakic, P. (2007). Notch regulates cell fate and dendrite morphology of newborn neurons in the postnatal dentate gyrus. *Proc. Natl. Acad. Sci. USA* **104**, 20558-20563. doi:10.1073/pnas.0710156104
Campbell, W. A., Yang, H., Zetterberg, H., Baulac, S., Sears, J. A., Liu, T., Wong, S. T., Zhong, T. P. and Xia, W. (2006). Zebrafish lacking Alzheimer presenilin enhancer 2 (Pen-2) demonstrate excessive p53-dependent apoptosis and neuronal loss. *J. Neurochem.* **96**, 1423-1440. doi:10.1111/j.1471-4159.2006.03648.x
Cheng, S., Liu, T., Hu, Y., Xia, Y., Hou, J., Huang, C., Zou, X., Liang, J., Stone Shi, Y., Zheng, Y. et al. (2019). Conditional inactivation of Pen-2 in the developing neocortex leads to rapid switch of apical progenitors to basal progenitors. *J. Neurosci.* **39**, 2195-2207. doi:10.1523/JNEUROSCI.2523-18.2019
Connor, S. E. J., Ng, V., McDonald, C., Schulze, K., Morgan, K., Dazzan, P. and Murray, R. M. (2004). A study of hippocampal shape anomaly in schizophrenia and in families multiply affected by schizophrenia or bipolar disorder. *Neuroradiol* **46**, 523-534. doi:10.1007/s00234-004-1224-0
De Strooper, B. (2003). Aph-1, Pen-2, and nicastrin with presenilin generate an active gamma-secretase complex. *Neuron* **38**, 9-12. doi:10.1016/S0896-6273(03)00205-8
Ehm, O., Goritz, C., Covic, M., Schaffner, I., Schwarz, T. J., Karaca, E., Kempkes, B., Kremmer, E., Pfrieger, F. W., Espinosa, L. et al. (2010). RBPJkappa-dependent signaling is essential for long-term maintenance of neural stem cells in the adult hippocampus. *J. Neurosci.* **30**, 13794-13807. doi:10.1523/JNEUROSCI.1567-10.2010
Forzano, F., Napoli, F., Uliana, V., Malacarne, M., Viaggi, C., Bloise, R., Coviello, D., Di Maria, E., Olivieri, I., Di Iorgi, N. et al. (2012). 19q13 microdeletion syndrome: Further refining the critical region. *Eur. J. Med. Genet.* **55**, 429-432. doi:10.1016/j.ejmg.2012.03.002
Fukumori, A. and Steiner, H. (2016). Substrate recruitment of gamma-secretase and mechanism of clinical presenilin mutations revealed by photoaffinity mapping. *EMBO J.* **35**, 1628-1643. doi:10.15252/embj.201694151
Galichet, C., Guillemot, F. and Parras, C. M. (2008). Neurogenin 2 has an essential role in development of the dentate gyrus. *Development* **135**, 2031-2041. doi:10.1242/dev.015115
Gana, S., Veggiotti, P., Sciacca, G., Fedeli, C., Bersano, A., Micieli, G., Maghnie, M., Ciccone, R., Rossi, E., Plunkett, K. et al. (2012). 19q13.11 cryptic deletion: description of two new cases and indication for a role of WTIP haploinsufficiency in hypospadias. *Eur. J. Hum. Genet.* **20**, 852-856. doi:10.1038/ejhg.2012.19
Guillemot, F. (2007). Cell fate specification in the mammalian telencephalon. *Prog. Neurobiol.* **83**, 37-52. doi:10.1016/j.pneurobio.2007.02.009
Hou, J., Bi, H., Ye, Z., Huang, W., Zou, G., Zou, X., Shi, Y., Shen, Y., Ma, Q., Kirchhoff, F. et al. (2021). Pen-2 negatively regulates the differentiation of oligodendrocyte precursor cells into astrocytes in the central nervous system. *J. Neurosci.* **41**, 4976-4990. doi:10.1523/JNEUROSCI.2455-19.2021
Houser, C. R. (1990). Granule cell dispersion in the dentate gyrus of humans with temporal lobe epilepsy. *Brain Res.* **535**, 195-204. doi:10.1016/0006-8993(90)91601-C
Huang, C., Liu, T., Wang, Q., Hou, W., Zhou, C., Song, Z., Shi, Y. S., Gao, X., Chen, G., Yin, Z. et al. (2020). Loss of PP2A disrupts the retention of radial glial progenitors in the telencephalic niche to Impair the generation for late-born neurons during cortical development. *Cereb. Cortex* **30**, 4183-4196. doi:10.1093/cercor/bhaa042
Imayoshi, I. and Kageyama, R. (2014). bHLH factors in self-renewal, multipotency, and fate choice of neural progenitor cells. *Neuron* **82**, 9-23. doi:10.1016/j.neuron.2014.03.018
Imayoshi, I., Shimogori, T., Ohtsuka, T. and Kageyama, R. (2008). Hes genes and neurogenin regulate non-neural versus neural fate specification in the dorsal telencephalic midline. *Development* **135**, 2531-2541. doi:10.1242/dev.021535
Langston, R. F. and Wood, E. R. (2009). Associative recognition and the hippocampus: Differential effects of hippocampal lesions on object-place, object-context and object-place-context memory. *Hippocampus* **20**, 1139-1153. doi:10.1002/hipo.20714
Lavado, A. and Oliver, G. (2014). Jagged1 is necessary for postnatal and adult neurogenesis in the dentate gyrus. *Dev. Biol.* **388**, 11-21. doi:10.1016/j.ydbio.2014.02.004
Lavado, A., Lagutin, O. V., Chow, L. M. L., Baker, S. J. and Oliver, G. (2010). Prox1 is required for granule cell maturation and intermediate progenitor maintenance during brain neurogenesis. *PLoS Biol.* **8**, e1000460. doi:10.1371/journal.pbio.1000460
Liu, M., Pereira, F. A., Price, S. D., Chu, M.-J., Shope, C., Himes, D., Eatock, R. A., Brownell, W. E., Lysakowski, A. and Tsai, M.-J. (2000a). Essential role of BETA2/NeuroD1 in development of the vestibular and auditory systems. *Genes Dev.* **14**, 2839-2854. doi:10.1101/gad.840500
Liu, M., Pleasure, S. J., Collins, A. E., Noebels, J. L., Naya, F. J., Tsai, M. J. and Lowenstein, D. H. (2000b). Loss of BETA2/NeuroD leads to malformation of the dentate gyrus and epilepsy. *Proc. Natl. Acad. Sci. U.S.A.* **97**, 865-870. doi:10.1073/pnas.97.2.865
Liu, T.-T., Ye, X.-L., Zhang, J.-P., Yu, T.-T., Cheng, S.-S., Zou, X.-C., Xu, Y., Chen, G.-Q. and Yin, Z.-Y. (2017). Increased adult neurogenesis associated with reactive astrocytosis occurs prior to neuron loss in a mouse model of neurodegenerative disease. *CNS Neurosci. Ther.* **23**, 885-893. doi:10.1111/cns.12763
Liu, Z. X., Yan, M. B., Liang, Y. J., Liu, M., Zhang, K., Shao, D. D., Jiang, R. C., Li, L., Wang, C. M., Nussenzveig, D. R. et al. (2019). Nucleoporin Seh1 interacts with Olig2/Brd7 to promote oligodendrocyte differentiation and myelination. *Neuron* **102**, 587-601.e7. doi:10.1016/j.neuron.2019.02.018
Lurton, D., Sundstrom, L., Brana, C., Bloch, B. and Rougier, A. (1997). Possible mechanisms inducing granule cell dispersion in humans with temporal lobe epilepsy. *Epilep. Res.* **26**, 351-361. doi:10.1016/S0920-1211(96)01002-9
Martin, S. J. and Clark, R. E. (2007). The rodent hippocampus and spatial memory: from synapses to systems. *Cell. Mol. Life Sci.* **64**, 401. doi:10.1007/s00018-007-6336-3
Martin, S. J., Grimwood, P. D. and Morris, R. G. M. (2000). Synaptic plasticity and memory: an evaluation of the hypothesis. *Ann. Rev. Neurosci.* **23**, 649-711. doi:10.1146/annurev.neuro.23.1.649
Miyata, T., Maeda, T. and Lee, J. E. (1999). NeuroD is required for differentiation of the granule cells in the cerebellum and hippocampus. *Genes Dev.* **13**, 1647-1652. doi:10.1101/gad.13.13.1647
Morrow, E. M., Furukawa, T., Lee, J. E. and Cepko, C. L. (1999). NeuroD regulates multiple functions in the developing neural retina in rodent. *Development* **126**, 23-36. doi:10.1242/dev.126.1.23
Muzumdar, M. D., Tasic, B., Miyamichi, K., Li, L. and Luo, L. (2007). A global double-fluorescent Cre reporter mouse. *Genesis* **45**, 593-605. doi:10.1002/dvg.20335
Nakahira, E. and Yuasa, S. (2005). Neuronal generation, migration, and differentiation in the mouse hippocampal primordium as revealed by enhanced green fluorescent protein gene transfer by means of in utero electroporation. *J. Comp. Neurol.* **483**, 329-340. doi:10.1002/cne.20441
O'Keefe, J. and Dostrovsky, J. (1971). The hippocampus as a spatial map. Preliminary evidence from unit activity in the freely-moving rat. *Brain Res.* **34**, 171-175. doi:10.1016/0006-8993(71)90358-1
Pleasure, S. J., Collins, A. E. and Lowenstein, D. H. (2000). Unique expression patterns of cell fate molecules delineate sequential stages of dentate gyrus development. *J. Neurosci.* **20**, 6095-6105. doi:10.1523/JNEUROSCI.20-16-06095.2000
Schwab, M. H., Bartholomae, A., Heimrich, B., Feldmeyer, D., Druffel-Augustin, S., Goebbels, S., Naya, F. J., Zhao, S. T., Frotscher, M., Tsai, M. J. et al. (2000). Neuronal basic helix-loop-helix proteins (NEX and BETA2/Neuro D) regulate terminal granule cell differentiation in the hippocampus. *J. Neurosci.* **20**, 3714-3724. doi:10.1523/JNEUROSCI.20-10-03714.2000
Shah, S., Lee, S.-F., Tabuchi, K., Hao, Y.-H., Yu, C., LaPlant, Q., Ball, H., Dann, C. E., Sudhof, T. and Yu, G. (2005). Nicastrin functions as a gamma-secretase-substrate receptor. *Cell* **122**, 435-447. doi:10.1016/j.cell.2005.05.022
Tamminga, C. A., Stan, A. D. and Wagner, A. D. (2010). The hippocampal formation in schizophrenia. *Am. J. Psychiat.* **167**, 1178-1193. doi:10.1176/appi.ajp.2010.09081187
Walton, N. M., Zhou, Y., Kogan, J. H., Shin, R., Webster, M., Gross, A. K., Heusner, C. L., Chen, Q., Miyake, S., Tajinda, K. et al. (2012). Detection of an immature dentate gyrus feature in human schizophrenia/bipolar patients. *Transl. Psychiat.* **2**, e135-e135. doi:10.1038/tp.2012.56
Wang, H., Liu, M., Ye, Z., Zhou, C., Bi, H., Wang, L., Zhang, C., Fu, H., Shen, Y., Yang, J. et al. (2021a). Akt regulates Sox10 expression to control oligodendrocyte

differentiation via phosphorylating FoxO1. *J. Neurosci.* **41**, 8163-8180. doi:10.1523/JNEUROSCI.2432-20.2021

Wang, H., Liu, M., Zou, G., Wang, L., Duan, W., He, X., Ji, M., Zou, X., Hu, Y., Yang, J. et al. (2021b). Deletion of PDK1 in oligodendrocyte lineage cells causes white matter abnormality and myelination defect in the central nervous system. *Neurobiol. Dis.* **148**, 105212. doi:10.1016/j.nbd.2020.105212

Wood, E. R. and Dudchenko, P. A. (2021). Navigating space in the mammalian brain. *Science* **372**, 913-914. doi:10.1126/science.abi9663

Wood, E. R., Dudchenko, P. A., Robitsek, R. J. and Eichenbaum, H. (2000). Hippocampal neurons encode information about different types of memory episodes occurring in the same location. *Neuron* **27**, 623-633. doi:10.1016/S0896-6273(00)00071-4

Zhuo, L., Theis, M., Alvarez-Maya, I., Brenner, M., Willecke, K. and Messing, A. (2001). hGFAP-cre transgenic mice for manipulation of glial and neuronal function in vivo. *Genesis* **31**, 85-94. doi:10.1002/gene.10008

Zou, Y., Jiang, W. X., Wang, J. Q., Li, Z. P., Zhang, J. Y., Bu, J. C., Zou, J., Zhou, L., Yu, S. Y., Cui, Y. Y. et al. (2014). Oligodendrocyte precursor cell-intrinsic effect of Rheb1 controls differentiation and mediates mTORC1-dependent myelination in brain. *J. Neurosci.* **34**, 15764-15778. doi:10.1523/JNEUROSCI.2267-14.2014

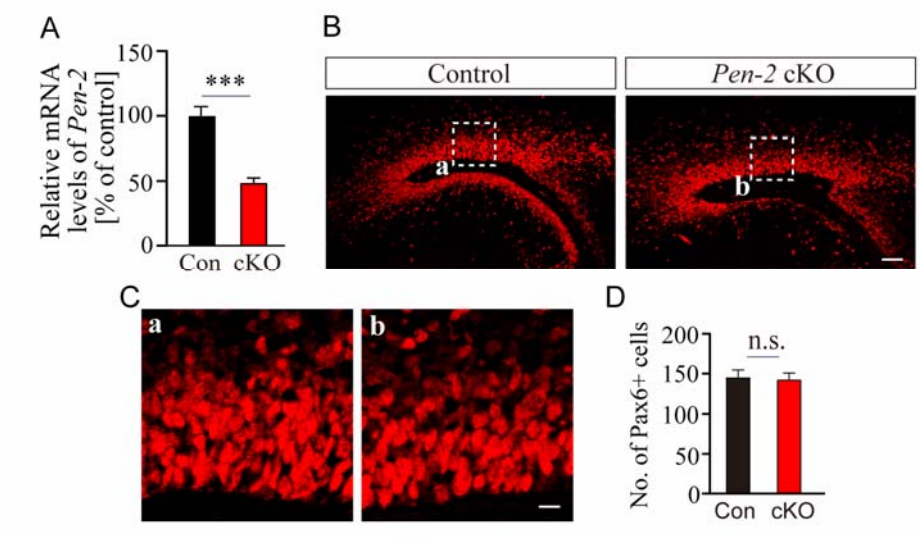

Fig. S1. Unchanged population of APs in the *Pen-2* cKO cortices.

A. Relative mRNA levels of *Pen-2* in the cortex at E16.5. There was significant difference between control and *Pen-2* cKO mice (***, $p<0.001$).

B. Representative fluorescence images for IHC on Pax6 in the cortex of *Pen-2* cKO mice at E17.5.

C. Enlarged images from the boxed areas in (B).

D. Averaged number of Pax6+ cells in the cortex. There was no significant difference between control and *Pen-2* cKO mice at E17.5 ($p>0.6$; n=3 embryos per group; n.s., not significant).

Scale bar is 50 μm in (A) or 10 μm in (B).

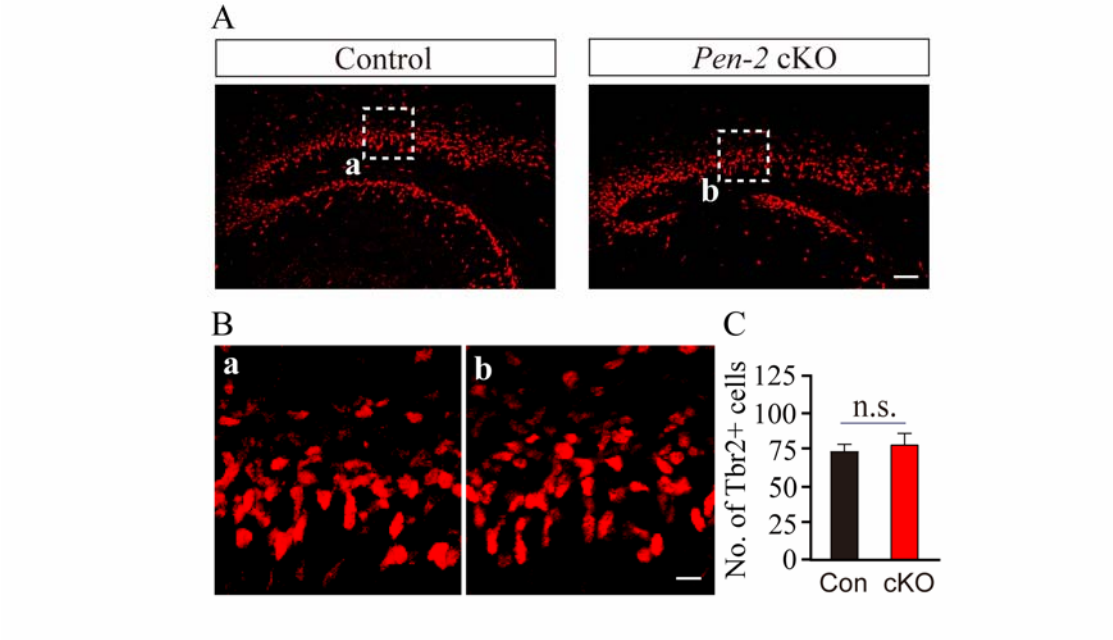

Fig. S2. Unchanged population of BPs in the *Pen-2* cKO cortices.

A. Representative fluorescence images for IHC on Tbr2 in the cortex of *Pen-2* cKO mice at E17.5.

B. Enlarged images from the boxed areas in (A).

C. Averaged number of Tbr2+ cells in the cortex. There was no significant difference between control and *Pen-2* cKO mice at E17.5 ($p>0.4$; n=3 embryos per group; n.s., not significant).

Scale bar is 50 μm in (A) or 10 μm in (B).

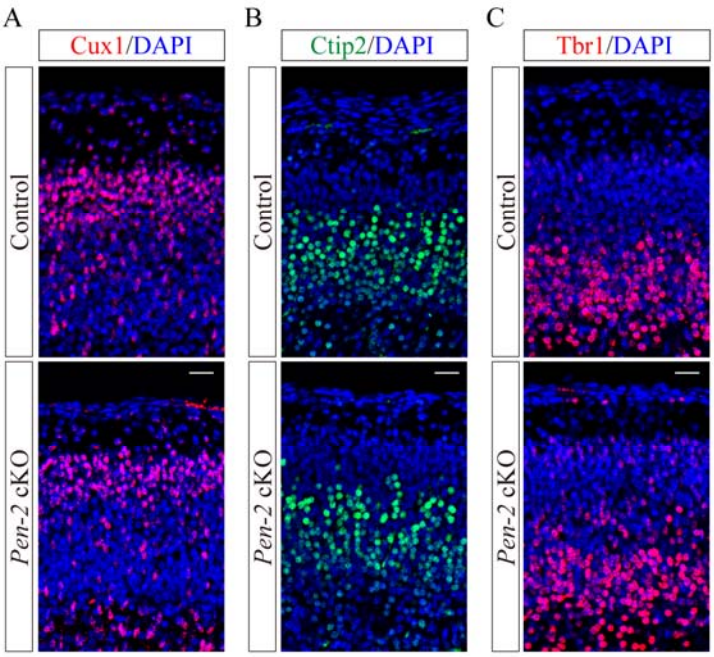

Fig. S3. Unaffected cortical lamination in *Pen-2* cKO mice.

Representative images for IHC on Cux1 (A), Ctip2 (B) and Tbr1 (C) in the cortex of *Pen-2* cKO mice at E17.5. There was no detectable difference on the immuno-reactivity of Cux1, Ctip2 or Tbr1 in the cortex between control and *Pen-2* cKO mice. Scale bar is 25 μm in (A), (B) or (C).

Table S1. Antibody list

Antibody	Source	Catalog No.	RRID No.
Rb anti-Pen2	ABclonal	A15172	AB_2762062
Rb anti-PS1 (loop,a.a.275-367,CT)	Merck	AB5308	RRID:AB_91785
Ms anti-GAPDH	CWbio	200306-7E4	AB_2722713
Rb anti-APP, C-terminus	Sigma-Aldrich	A8717	AB_258409
Goat anti-Sox2	Santa Cruz Biotechnology	sc-17320	AB_2286684
Goat anti-Prox1	R&D Systems	AF2727	2170716
Rb anti-Pax6	Biolegend	901301	AB_2565003
Rb anti-Tbr2	Abcam	ab23345	AB_778267
Rb anti-Tbr1	Abcam	ab183032	Not available
Rat anti-BrdU	Abcam	ab6326	AB_305426
Rb anti-CC3(Cleaved caspase-3)	Cell Signaling Technology	#9661	AB_2341188
Ms anti-NeuroD1	Abcam	ab60704	AB_943491